Antiviral Research 85 (2010) 520–524

Contents lists available at ScienceDirect

Antiviral Research

journal homepage: www.elsevier.com/locate/antiviral

Identification of hepatitis C virus genotype 2a replicon variants with reduced susceptibility to ribavirin

Su Su Hmwe[a,b], Hideki Aizaki[a], Tomoko Date[a], Kyoko Murakami[a], Koji Ishii[a], Tatsuo Miyamura[a], Kazuhiko Koike[b], Takaji Wakita[a], Tetsuro Suzuki[a,*]

[a] Department of Virology II, National Institute of Infectious Diseases, 1-23-1 Toyama, Shinjuku-ku, Tokyo 162-8640, Japan
[b] Department of Gastroenterology, Graduate School of Medicine, University of Tokyo, 7-3-1 Hongo, Bunkyo-ku, Tokyo 113-8655, Japan

ARTICLE INFO

Article history:
Received 8 April 2009
Received in revised form 19 October 2009
Accepted 18 December 2009

Keywords:
Hepatitis C virus
Replication
Ribavirin
Drug resistance

ABSTRACT

Ribavirin (RBV), a nucleoside analogue, is used in the treatment of hepatitis C virus (HCV) infection in combination with interferons. However, potential mechanisms of RBV resistance during HCV replication remain poorly understood. Serial passage of cells harboring HCV genotype 2a replicon in the presence of RBV resulted in the reduced susceptibility of the replicon to RBV. Transfection of fresh cells with RNA from RBV-resistant replicon cells demonstrated that the RBV resistance observed is largely replicon-derived. Four major amino acid substitutions: T1134S in NS3, P1969S in NS4B, V2405A in NS5A, and Y2471H in NS5B region, were identified. Site-directed mutagenesis of these mutations into the replicon indicated that Y2471H plays a role in the reduced susceptibility to RBV and leads to decrease in replication fitness. The results, in addition to analysis of sequence database, suggest that HCV variants with reduced susceptibility to RBV identified are preferential to genotype 2a.

1. Introduction

Hepatitis C virus (HCV) is a leading cause of chronic liver diseases, such as chronic hepatitis, cirrhosis and hepatocellular carcinoma, affecting approximately 170 million people worldwide (WHO, 2000). HCV belongs to the genus Hepacivirus of the family Flaviviridae, and its genome is a single-stranded, positive-sense RNA of 9.6 kb. HCV displays marked genetic heterogeneity and is currently classified into 6 major genotypes and more than 50 subtypes. HCV genotypes have regional distribution and, of those, genotypes 1 and 2 are detected worldwide (Simmonds et al., 2000). Current standard therapy for chronic hepatitis C consists of the combination of pegylated interferon alpha (IFN-α) in combination with ribavirin (RBV). However, approximately 50% of treated patients infected with genotype 1 do not respond or show only a partial or transient response and treatment is limited by the adverse effects of both agents (Manns et al., 2001; Fried et al., 2002).

HCV replication is associated with a high rate of mutation that gives rise to a mixed and changing population of mutants, known as quasispecies (Martell et al., 1992; Domingo, 1996). The characteristic of HCV may have important implications concerning viral persistence, pathogenicity and resistance to antiviral agents (Domingo, 1996; Forns et al., 1999; Farci and Purcell, 2000). Most previous studies on the possible relationship between HCV quasispecies and response to chemotherapy have been carried out in HCV genotype 1 patients. In addition, several studies have successfully demonstrated that the HCV subgenomic replicon is derived from genotype 1, which typically contains HCV nonstructural genes placed downstream of the neomycin phosphotransferase gene, in selecting variants resistant to antiviral inhibitors. Two studies have demonstrated the identification of HCV genotype 1 mutants responsible for decreased sensitivity to RBV (Young et al., 2003; Pfeiffer and Kirkegaard, 2005). However, little is known about the generation of genotype 2 isolates resistant to antivirals including RBV, or the molecular mechanisms that confer resistance.

In this study, we report the generation and characterization of HCV genotype 2a replicon variants with reduced susceptibility to RBV. The impacts of major amino acid substitutions observed on RBV susceptibility and viral replication capacity were also examined.

2. Materials and methods

2.1. Compounds

RBV and IFN-α were purchased from MP Biomedicals (Eschwege, Germany) and Dainippon Sumitomo Pharma (Osaka, Japan), respectively.

* Corresponding author. Tel.: +81 3 5285 1111; fax: +81 3 5285 1161.
E-mail address: tesuzuki@nih.go.jp (T. Suzuki).

0166-3542/$ – see front matter © 2010 Elsevier B.V. All rights reserved.
doi:10.1016/j.antiviral.2009.12.008

Table 1
Primers used for PCR and nucleotide sequencing.

Region	Primer name	Nucleotide sequence	Position[a]	Polarity
NS3–4A–4B region	PCR primers			
	JF1S	GAAAAACACGATGATACCATG	1756–1776	Sense
	JF1AS	AACCCAGTCCCACACGTC	4650–4633	Antisense
	Sequencing primers			
	JF5S	CACTTTCAGTGACAACAGCA	2322–2341	Sense
	JF6S	CGCCACCGACGCCCTCATGA	3003–3022	Sense
	JF4AS	CTGGTCGACAACGGACTGGT	4109–4090	Antisense
NS5A–NS5B region	PCR primers			
	JF2S	TGCTCCGGATCCTGGCTC	4612–4629	Sense
	JF2AS	TACCTAGTGTGTGCCGCTCTA	7786–7806	Antisense
	Sequencing primers			
	JF3S	TGAGGTCCATGCTAACAGA	5209–5228	Sense
	JF4S	TCGAGGGGGAGCCTGGAGAT	5870–5889	Sense
	JF3AS	GAGTGTCTAACTGTTTCCCAG	7220–7200	Antisense

[a] Reference strain: Gene Bank accession no. AB114136.

2.2. Cell culture

The human hepatoma cell line Huh-7 was maintained in Dulbecco's modified Eagle's medium (DMEM) supplemented with MEM non-essential amino acids (Invitrogen) 100 units/ml penicillin, 100 μg/ml streptomycin, and 10% fetal bovine serum (FBS) at 37 °C in a 5% CO_2 incubator. HCV replicon cells JFH-1/4-1 (Miyamoto et al., 2006), which are Huh-7-derived cells carrying a subgenomic replicon of JFH-1 (Kato et al., 2003) were maintained in the Huh-7 medium as above, supplemented with 1 mg/ml G418 (Nacalai Tesque, Kyoto, Japan).

2.3. Quantification of HCV RNA

Total RNA was isolated from harvested cells using Trizol (Invitrogen). Copy numbers of the viral RNA were determined by real-time RT-PCR involving single-tube reactions and performed using TaqMan EZ RT-PCR Core Reagents (PE Applied Biosystems, Foster City, CA, USA), as described previously (Aizaki et al., 2003; Takeuchi et al., 1999).

2.4. Cell viability assay

Cells were seeded at density of 5×10^4 cells/well in 24-well plates and RBV at various concentrations was added on the next day. Cultures were further incubated for 3 days at 37 °C under a humidified 5% CO_2 atmosphere. Cytotoxicity assay was performed by Cell Titer-GLO™ Luminescent Cell Viability Assay (Promega, Madison, WI, USA) according to the manufacturer's instructions. Luciferase activities were quantified with LUMAT LB 9501 (Berthold Technologies, Bad Wilbad, Germany).

2.5. Isolation and nucleotide sequencing of HCV nonstructural regions from replicon-containing cells

Total cellular RNA was isolated from replicon cells with or without RBV treatment as described above. cDNA synthesis was carried out by using Super ScriptTM III First-Strand Synthesis System for RT-PCR (Invitrogen) with primer JF1AS for NS34AB region and JF2AS for NS5AB region. Two cDNA fragments, corresponding to NS3–NS4B and NS5A–NS5B regions, were amplified by PCR using Takara EX Taq DNA polymerase (Takara BIO, Kyoto, Japan) and specific primers (Table 1; Date et al., 2004). PCR products were subcloned into pGEM-T vector (Promega) and inserts were sequenced using QIA prep^R Spin Mini Prep kit (QIAGEN, Tokyo, Japan). Nucleotide sequences were analyzed with the 3100 Avant Genetic Analyzer (PE Applied Biosystems).

2.6. Plasmid constructions

pSGR-JFH1/luc, a subgenomic replicon construct with luciferase reporter derived from HCV genotype 2a JFH-1 isolate was reported previously (Miyamoto et al., 2006). Mutant replicons carrying T1134S, P1969S, V2405A, and Y2471H were created by PCR-based site-directed mutagenesis and cDNA fragments containing the above mutations were inserted into the corresponding sites of pSGR-JFH/luc. All plasmids were confirmed by sequencing the entire PCR-generated inserts. Each mutant is referred to by the original amino acid (one letter code) followed by the residue positions within the complete open reading frame of full-length JFH-1 and the substituted amino acid (one letter code).

2.7. RNA synthesis and transient replication assay

The transient replication assay method was described previously (Kato et al., 2005). Briefly, purified plasmids of pSGR-JFH1/Luc, -JFH1/Luc-T1134S, -JFH/Luc-P1969S, -JFH/Luc-V2405A and -JFH/Luc-Y2471H were linearized with XbaI and were treated with proteinase K and SDS, followed by phenol–chloroform extraction. RNA was synthesized with Ampliscribe™ T7 Transcription Kits (Epicentre BIO Technologies, Madison, WI, USA). Each transcribed RNA (5 μg) was electroporated into 2.5×10^6 of Huh7 cells pulsed at 290 mV, 975uFD with Gene pulser II apparatus (Bio-Rad Laboratories, Hercules, CA, USA). Transfected cells were resuspended in growth medium without selection antibiotics and were plated in 24-well plates at 6×10^4 cells per well. Cells were harvested at different time points post-transfection and were lysed in Passive Lysis Buffer (Promega). Luciferase activity in cells was determined using the Luciferase Assay System (Promega).

3. Results

3.1. Selection of replicon variants derived from genotype 2a with reduced susceptibility to RBV

It has been reported that RBV inhibits HCV RNA replication in Huh-7 cells bearing the viral subgenomic replicon RNAs with the EC_{50} (50% effective concentration) values of 15–225 μM (Zhou et al., 2003; Tanaka et al., 2004; Kato et al., 2005; aus dem Siepen et al., 2007). To select for RBV-associated replicon variants, cells bearing a genotype 2a HCV replicon were serially passed in the presence of 200 μM RBV as well as 1 mg/ml G418. After 20-week treatment, variant cells were then tested for RBV resistance. HCV RNA levels were determined after a 72-h incubation with various concentrations of RBV in the absence of G418, and about 5-fold-reduced susceptibility to RBV was observed in the variant replicon

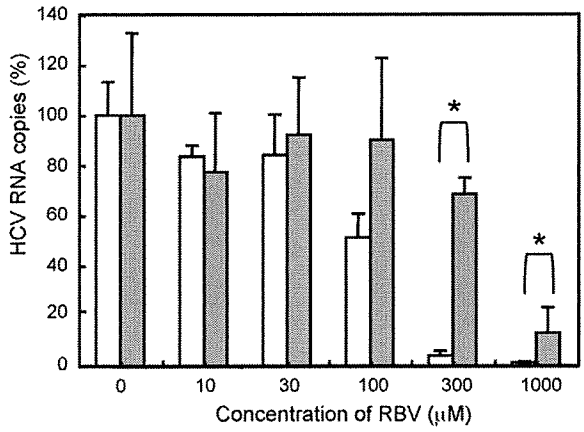

Fig. 1. Inhibitory effect of RBV on HCV RNA levels in genotype 2a replicon cells after long-term treatments with RBV. The replicon cells were serially passaged in 0 or 200 μM RBV for 20 weeks. The cells were then split and incubated with fresh RBV at various concentrations in the absence of G418 for 3 days, followed by the determination of HCV RNA. Clear bars, passage in the absence of RBV: gray bars, passage in the presence of RBV. HCV RNA copies per microgram of total RNA were normalized as percentages of those of untreated (RBV 0 μM). Each data point is presented as the mean of three independent determinations with standard deviation. $^*p < 0.05$.

cells; the EC_{50} values for the variant and wild-type replicon cells were 470 and 102 μM, respectively (Fig. 1). Comparable cytotoxic effects of RBV were observed against wild-type and variant replicon cells, with the CC_{50} (50% cytotoxicity concentration) values of 151 and 156 μM, respectively (data not shown).

3.2. Mapping RBV resistance to cell line or replicon RNA

To test whether reduced susceptibility to RBV in the variant cells observed as above was due to the appearance of mutations within the viral RNA or was cell-derived, total RNAs from the variant and wild-type replicon cells were extracted and used for retransfection of naïve Huh7 cells. Retransfected cells resistant to G418 were established after 4 weeks of cultures in the presence of 1 mg/ml G418 and were assessed for HCV RNA replication sensitivity to RBV (Fig. 2A). HCV RNA levels in the cells obtained from the wild-type replicon were inhibited by 56, 89 and 97% with 100, 300 and 1000 μM RBV, respectively. By contrast, the culture retransfected with RNA derived from the variant replicon cells exhibited inhibition levels of 13, 29 and 89% with the corresponding concentrations of RBV. EC_{50} values were calculated to be 93 and 449 μM, respectively. We confirmed the presence of replicon mutations, as described below, in the cells retransfected with RNA derived from the variant replicon cells.

In order to explore the possibility for cell-derived resistance, both wild-type and variant replicon cells were cured of viral RNAs by IFN treatment; cells were passaged with media containing 100 IU/mL IFN-α in the absence of G418 for 2 months. To compare RBV sensitivity, cured cells were transiently transfected with the wild-type JFH-1 subgenomic replicon RNA and were treated with various concentrations of RBV for 72 h. Similar anti-HCV effects of RBV were observed in the cured cells derived from wild-type and variant replicons, with the EC_{50} values of 147 and 118 μM, respectively (Fig. 2B). Thus, the results suggest that the RBV resistance observed may arise by mutations in the replicon rather than by changes in the cells.

3.3. HCV mutations in replicon variant with reduced susceptibility to RBV

It has been reported that mutations in RNA virus genomes responsible for RBV resistance are mostly present in the coding region for the viral RNA-dependent RNA polymerase (RdRp). On the other hand, it is known that RBV works as an RNA mutagen to generate rapidly mutating viral RNA and that NS5B RdRp and other nonstructural proteins in HCV are involved in the viral replication complex, playing key roles in genome replication. Therefore, we sequenced the coding regions for NS3 through NS5B proteins of the replicon molecules in order to determine whether mutations associated with RBV resistance were generated. As shown in Table 2, there were numerically more synonymous and non-synonymous mutations in the RBV-resistant variant replicon cells (RBV treatment) when compared with untreated replicative conditions (No-treatment) across most regions examined. Mutation frequencies of NS3, NS4B and NS5A regions of RBV treatment were significantly higher than those of No-treatment. The total number of synonymous mutations in the RBV-resistant variant replicon cells was 3 times higher than that under untreated replicative conditions, and the number of non-synonymous mutations in the RBV-resistant variant replicon cells was 1.5 times higher than that under untreated replicative conditions. The number of both synonymous and non-synonymous mutations (NS3, NS4B, NS5A and NS5B regions) in the RBV-resistant replicon cells was greater than that in the control cells. We also found a large number of transition

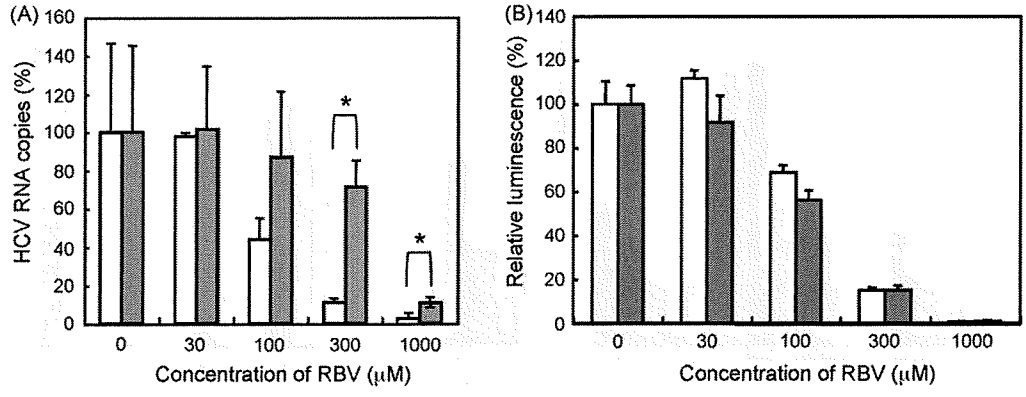

Fig. 2. Testing for replicon-derived resistance (A) or for cell-derived resistance (B). (A) Total RNA from RBV-resistant- or wild-type replicon cells was transfected into naïve Huh7 cells. After selection in 1 mg/ml G418 for 4 weeks, re-established replicon cells, wild-type derived (clear bars) and RBV resistance derived (gray bars), were treated with increasing concentrations of RBV in the absence of G418 for 3 days. HCV RNA copies per microgram total RNA were assessed and the levels from wild-type cells without RBV treatment were set at 100%. Data are indicated as means with standard deviations. $^*p < 0.05$. (B) RBV-resistant- or wild-type replicon cells were cured by passage in IFN-α in the absence of G418. Cured cells were transiently transfected with the replicon RNA derived from pSGR-JFH1/luc. Transient replication assay of transfectants derived from wild-type (clear bars) and RBV resistance (gray bars) was performed after treatment with various concentrations of RBV for 72 h. The values for wild-type-derived cells without RBV treatment were set at 100%. Data are indicated as means with standard deviations.

Table 2
Mutation frequencies in HCV NS regions after 20-weeks culture with or without RBV treatment.

Region	nt length	No-treatment			RBV treatment		
		No. of non-synonymous mutations[a]	No. of synonymous mutations[a]	Mutation frequency (10^{-3})	No. of non-synonymous mutations[a]	No. of synonymous mutations[a]	Mutation frequency (10^{-3})
NS3	1893	1.7 ± 2.1	2.3 ± 1.5	2.1	4.7 ± 2.4	6.5 ± 2.5	5.9[b]
NS4A	165	1.0 ± 1.0	0.3 ± 0.6	8.1	0.3 ± 0.5	0.5 ± 0.9	4.4
NS4B	780	1.3 ± 1.2	0.3 ± 0.6	2.1	2.3 ± 1.5	2.5 ± 1.2	4.7[c]
NS5A	1380	4.0 ± 1.2	2.0 ± 1.2	4.3	5.9 ± 1.2	6.2 ± 2.4	12.2[c]
NS5B	1773	4.5 ± 1.5	2.3 ± 1.5	3.8	4.8 ± 1.8	4.2 ± 1.1	9.0
NS3–NS5B	5991	12.5 ± 2.7	7.3 ± 2.7	–	17.8 ± 4.5	20.1 ± 4.6	–

[a] Values are means ± standard deviations.
[b] $p < 0.05$ relative to No-treatment by the unpaired t-test.
[c] $p < 0.01$ relative to No-treatment by the unpaired t-test.

mutations in RBV-resistant cells, particularly G-to-A and C-to-U transitions, as expected from previous studies. Although mutations were distributed throughout nonstructural regions, four major amino acid substitutions; T1134S in the NS3 region, P1969S in NS4B, V2405A in NS5A, and Y2471H in NS5B, not seen in wild-type cells were observed in most of the subclones among RBV-resistant replicon cells. T1134S, P1969S, V2405A, and Y2471H were present, respectively, in 7 of 11, 6 of 11, 8 of 13, and 7 of 13 PCR subclones sequenced.

3.4. Effects of T1134S, P1969S, V2405A, and Y2471H on RBV susceptibility

To test the possibility that any of the four mutations as identified confer resistance to RBV, we introduced these mutations individually into the JFH-1 subgenomic replicon containing a luciferase reporter gene. Cells transfected with mutant- or wild-type replicon RNA grown in the presence of various concentrations of RBV for 2 or 3 days. As demonstrated in Fig. 3A, the replication levels of all four mutant replicons (SGR-JFH1/Luc-T1134S, -P1969S, -V2405A, and -Y2471H) in the presence of 125 or 500 μM RBV were higher than those of the wild-type replicon. In particular, the Y2471H mutant significantly reduced susceptibility to RBV; replication levels of SGR-JFH1/Luc-Y2471H were 3–5-fold higher when compared to those of wild-type under the present assay conditions.

The relative replication activity of these mutant replicons was further determined in 3-day replication assay without drug treatment (Fig. 3B). All mutant replicons exhibited reduced efficiency relative to the wild-type replicon. Levels of the Y2471H-mutated replicon were approximately 30% of those of the wild-type, thus suggesting that replicon mutants with reduced sensitivity to RBV are associated with decreased replication fitness.

4. Discussion

It is generally accepted that, during chemotherapy against viral infection, high rates of viral replication and high frequencies of mutation lead to generation of drug-resistant mutants. Although several potential mechanisms for the inhibition of HCV replication by RBV have been proposed, the molecular mechanisms involved in the generation of RBV-resistant HCV remain poorly understood.

This study found that long-term treatment of HCV JFH-1-derived replicon cells with RBV leads to selection of preferential mutations in NS3 (T1134S), NS4B (P1969S), NS5A (V2405A) and NS5B (Y2471H) genes. Each mutation only required a single nucleotide change, and P1969S, V2405A and Y2471H are transition mutations, which are known to be commonly caused by incorporated RBV. Site-directed mutagenesis of these mutations into the replicon demonstrated that Y2471H plays a role in reduced susceptibility to RBV.

Crystal structure information revealed that HCV RdRp is organized into an arrangement with palm, fingers, and thumb subdomains (Lesburg et al., 1999). Residue 2471 (the 33rd position of NS5B) is present in the N-terminal loop region that bridges the fingers. Although this site is apparently distant from the active site of the polymerase in the palm region, it has been reported

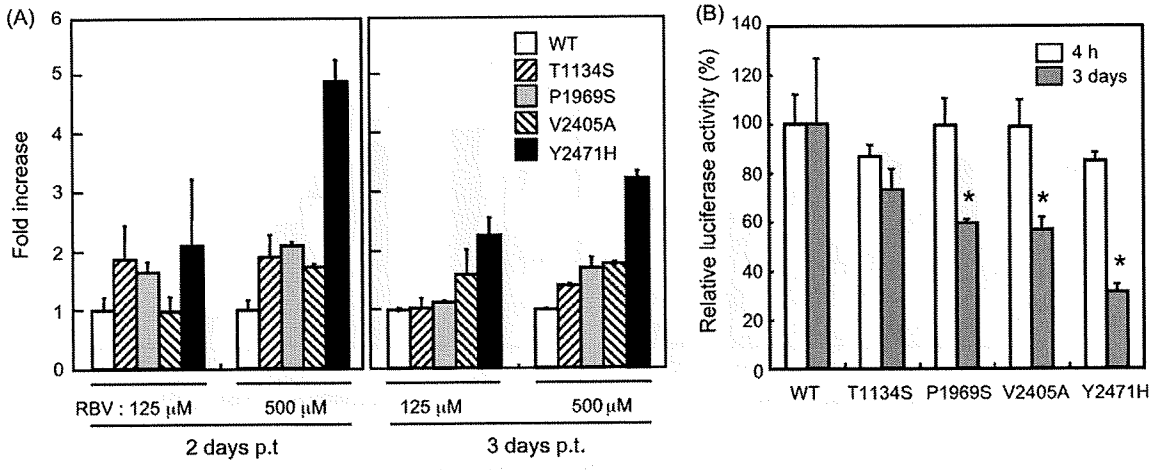

Fig. 3. Impact of major mutations in NS3–NS5B regions on RBV susceptibility (A) and replication capacity (B). Mutated replicons carrying single residue substitutions (T1134S, P1969S, V2405A, and Y2471H) were constructed and used for transient replication assay. Cells were transfected with either wild-type (WT) or with mutant replicon RNA in the absence or presence (125, 500 μM) of RBV. Luciferase activity was assessed at 4 h, 2 days and 3 days post-transfection (p.t.). (A) Luciferase activities of WT were set at 1, and the fold increases in the activities of mutants were plotted. (B) Luciferase activities in the absence of RBV at 4 h and 3 days post-transfection were shown. The activities of mutants were normalized as percentages of the WT activities. Data from triplicate samples were averaged and indicated with standard deviations. *$p < 0.05$ against WT.

that small molecules, such as benzimidazole compounds, are able to specifically bind the fingers-thumb interface and inhibit polymerase activity (Herlihy et al., 2008), thus suggesting that amino acid substitutions in the loop region may affect RNA polymerization. The involvement of tyrosine residue at position 415 of HCV NS5B in RBV resistance has been previously described for patients with genotype 1a infection and for the genotype 1b replicon (Young et al., 2003). Although the mechanism for resistance remains elusive, it has been hypothesized that RBV interacts with RdRp around this residue, which is located in the thumb subdomain, thus affecting RNA polymerization (Young et al., 2003).

Based on analysis of available sequences from Genbank, tyrosine at the 33rd residue of NS5B is conserved in all isolates of genotype 2a, but not in other genotypes. In genotype 1a and 1b isolates, 96% contain histidine and only a small population contains tyrosine or asparagine at the site. All the isolates of genotypes 3, 4, 5 and 6 contain histidine, whereas phenylalanine is conserved for genotype 2b. It should be noted that V2405 and P1969 are also completely conserved for genotype 2a but not for other genotypes. Therefore, it is likely that the identified HCV variants with reduced susceptibility to RBV are genotype-specific. It will be of interest to determine whether HCV genotype 2a is intrinsically more sensitive to RBV when compared with other genotypes.

At present, at least 4 mechanisms of action of RBV are proposed (Lau et al., 2002). They include (1) direct inhibition of the HCV replication machinery, (2) as an RNA mutagen that drives a rapidly mutating RNA virus over the threshold to "error catastrophe", (3) inhibition of the host enzyme inosine monophosphate dehydrogenase (IMPDH), and (4) enhancement of host T-cell-mediated immunity against viral infection. In addition to the direct inhibition, it is also possible that other mechanisms such as error-prone and IMPDH-inhibition are involved in HCV escape from RBV treatment. Further investigation of the interaction of HCV variants with the viral and cellular factors involved in viral resistance may improve understanding of the mechanism(s) of RBV resistance.

In conclusion, RBV encountered resistance from the HCV genotype 2a replicon largely mediated by mutations in the N-terminal region of NS5B. Although whether these mutagenic effects are also demonstrable in IFN-RBV combination therapy will require further studies, the mutations identified in this study represent the first drug-resistant variants belonging to HCV genotype 2a. The drug resistance patterns found in this study may be of benefit in prediction in vivo resistance profiles and the development of next-generation nucleoside analogues as anti-HCV drugs.

Acknowledgments

We thank M. Matsuda, S. Yoshizaki, M. Ikeda, T. Shimoji, M. Kaga and M. Sasaki for their technical assistance. This work was supported by a grant-in-aid for Scientific Research from the Japan Society for the Promotion of Science, from the Ministry of Health, Labour and Welfare of Japan and from the Ministry of Education, Culture, Sports, Science and Technology, and by Research on Health Sciences focusing on Drug Innovation from the Japan Health Sciences Foundation, Japan and by the Program for Promotion of Fundamental Studies in Health Sciences of the National Institute of Biomedical Innovation of Japan. S.S.H. is the recipient of a Research Resident Fellowship from Viral Hepatitis Research Foundation of Japan.

References

Aizaki, H., Nagamori, S., Matsuda, M., Kawakami, H., Hashimoto, O., Ishiko, H., Kawada, M., Matsuura, T., Hasumura, S., Matsuura, Y., Suzuki, T., Miyamura, T., 2003. Production and release of infectious hepatitis C Virus for human liver cell cultures in the three-dimensional radial-flow bioreactor. Virology 314, 16–25.

aus dem Siepen, M., Oniangue-Ndza, C., Wiese, M., Ross, S., Roggendorf, M., Viazov, S., 2007. Interferon-alpha and ribavirin resistance of Huh7 cells transfected with HCV subgenomic replicon. Virus Res. 125, 109–113.

Date, T., Kato, T., Miyamoto, M., Zhao, Z., Yasui, K., Mizokami, M., Wakita, T., 2004. Genotype 2a hepatitis C virus subgenomic replicon can replicate in HepG2 and IMY-N9 cells. J. Biol. Chem. 279, 22371–22376.

Domingo, E., 1996. Biological significance of viral quasispecies. Viral Hep. Rev. 2, 247–261.

Farci, P., Purcell, R.H., 2000. Clinical significance of hepatitis C virus genotypes and quasispecies. Semin. Liver Dis. 20, 103–126.

Forns, X., Purcell, R.H., Bukh, J., 1999. Quasispecies in viral persistence and pathogenesis of hepatitis C virus. Trends Microbiol. 7, 402–410.

Fried, T.R., Bradley, E.H., Towle, V.R., Allore, H., 2002. Understanding the treatment preferences of seriously ill patients. N. Engl. J. Med. 346, 1061–1066.

Herlihy, K.J., Graham, J.P., Kumpf, R., Patick, A.K., Duggal, R., Shi, S.T., 2008. Development of intragenotypic chimeric replicons to determine the broad-spectrum antiviral activities of hepatitis C virus polymerase inhibitors. Antimicrob. Agents Chemother. 52, 3523–3531.

Kato, T., Date, T., Miyamoto, M., Furusaka, A., Tokushige, K., Mizokami, M., Wakita, T., 2003. Efficient replication of the genotype 2a hepatitis C virus subgenomic replicon. Gastroenterology 125, 1808–1817.

Kato, T., Date, T., Miyamoto, M., Sugiyama, M., Tanaka, Y., Orito, E., Ohno, T., Sugihara, K., Hasegawa, I., Fujiwara, K., Ito, K., Ozasa, A., Mizokami, M., Wakita, T., 2005. Detection of anti-hepatitis C virus effects of interferon and ribavirin by a sensitive replicon system. J. Clin. Microbiol. 43, 5679–5684.

Lau, J.Y., Tam, R.C., Liang, T.J., Hong, Z., 2002. Mechanism of action of ribavirin in the combination treatment of chronic HCV infection. Hepatology 35, 1002–1009.

Lesburg, C.A., Cable, M.B., Ferrari, E., Hong, Z., Mannarino, A.F., Weber, P.C., 1999. Crystal structure of the RNA-dependent RNA polymerase from hepatitis C virus reveals a fully encircled active site. Nat. Struct. Biol. 6, 937–943.

Manns, M.P., McHutchison, J.G., Gordon, S.C., Rustgi, V.K., Shiffman, M., Reindollar, R., Goodman, Z.D., Koury, K., Ling, M., Albrecht, J.K., 2001. Peginterferon alfa-2b plus ribavirin compared with interferon alfa-2b plus ribavirin for initial treatment of chronic hepatitis C: a randomised trial. Lancet 358, 958–965.

Martell, M., Esteban, J.I., Quer, J., Genesca, J., Weiner, A., Esteban, R., Guardia, J., Gomez, J., 1992. Hepatitis C virus (HCV) circulates as a population of different but closely related genomes: quasispecies nature of HCV genome distribution. J. Virol. 66, 3225–3229.

Miyamoto, M., Kato, T., Date, T., Mizokami, M., Wakita, T., 2006. Comparison between subgenomic replicons of hepatitis C virus genotypes 2a (JFH-1) and 1b (con1 NK5.1). Intervirology 49, 37–43.

Pfeiffer, J.K., Kirkegaard, K., 2005. RBV resistance in hepatitis C virus replication containing cells conferred by changes in the cell line or mutations in the replicon RNA. J. Virol. 79, 2346–2355.

Simmonds, P., Gallin, J.I., Farrei, A.S., 2000. Hepatitis C virus genotypes. Biomed. Res. Rep. 2, 53–70.

Takeuchi, T., Katsume, A., Tanaka, T., Abe, A., Inoue, K., Tsukiyama Kohara, K., Kawaguchi, R., Tanaka, S., Kohara, M., 1999. Real-time detection system for quantification of Hepatitis C virus genome. Gastroenterology 116, 636–642.

Tanaka, Y., Sakamoto, N., Enomoto, N., Kurosaki, M., Ueda, E., Maekawa, S., Yamashiro, T., Nakagawa, M., Chen, C.-H., Kanazawa, N., Kakinuma, S., 2004. Synergistic inhibition of intracellular hepatitis C virus replication by combination of ribavirin and interferon-alpha. J. Infect. Dis. 189, 1129–1139.

World Health Organization (WHO), 2000. Hepatitis C: global prevalence (update). Weekly Epidemiological Record, WHO 75, 18–19.

Young, K.C., Lindsay, K.L., Lee, K.J., Liu, W.C., He, J.W., Milstein, S.L., Lai, M.M., 2003. Identification of a ribavirin-resistant NS5B mutation of hepatitis C virus during ribavirin monotherapy. Hepatology 38, 869–878.

Zhou, S., Liu, R., Baroudy, B.M., Malcolm, B.A., Reyes, G.R., 2003. The effect of ribavirin and IMPDH inhibitors on hepatitis C virus subgenomic replicon RNA. Virology 310, 333–342.

JOURNAL OF CLINICAL MICROBIOLOGY, Dec. 2009, p. 4141–4143 Vol. 47, No. 12
0095-1137/09/$12.00 doi:10.1128/JCM.01437-09

Evaluation of Hepatitis C Virus Core Antigen Assays in Detecting Recombinant Viral Antigens of Various Genotypes[▽]

Mohsan Saeed,[1,3] Ryosuke Suzuki,[1] Madoka Kondo,[1] Hideki Aizaki,[1] Takanobu Kato,[1] Toshiaki Mizuochi,[2] Takaji Wakita,[1] Haruo Watanabe,[1,3] and Tetsuro Suzuki[1]*

Department of Virology II[1] and Department of Safety Research on Blood and Biological Products,[2] National Institute of Infectious Diseases, Tokyo 162-8640, and Department of Infection and Pathology, Graduate School of Medicine, The University of Tokyo, Hongo, Bunkyo-ku, Tokyo 113-0033,[3] Japan

Received 24 July 2009/Returned for modification 3 September 2009/Accepted 19 September 2009

A single substitution within the hepatitis C virus core antigen sequence, A48T, which is observed in ~30% of individuals infected with genotype 2a virus, reduces the sensitivity of a commonly used chemiluminescence enzyme immunoassay. Quantitation of the antigen is improved by using a distinct anticore antibody with a different epitope.

Hepatitis C virus (HCV) is a major cause of chronic liver disease throughout the world. Accurate diagnosis of HCV infection is important due to the morbidity associated with the virus, and determining the level of viral replication is important in predicting and monitoring the effect of antiviral treatment. Although quantifying viral RNA represents the standard method for identifying active infection (5, 8, 13), several sensitive immunoassays that detect the viral core antigen (Ag) have now been developed as an alternative to HCV RNA testing (3, 4, 6, 9, 10, 12, 16). The amino acid sequence of the core Ag is largely conserved among different viral isolates (14); however, genetic variability of the virus constitutes one of the major challenges to using core Ag assays for diagnosis. In this study, we examined the effects of sequence heterogeneity on the sensitivity of diagnostic kits for detection of the core Ag by using recombinant Ag derived from each of the major HCV genotypes. Expression plasmids for epitope-tagged core Ag were generated by inserting cDNA for the full-length core region of genotype 1a (17; GenBank accession no. AF011751), 1b (1; D89815), 2a (7; AB047639), 2b (AB030907), or 3a virus, with a FLAG tag sequence attached at its 5′ end, into the EcoRI site of the pCAG mammalian expression vector (11). HEK293T cells transiently transfected with the expression plasmids were harvested 48 h after transfection using a passive lysis buffer (Promega, Madison, WI). Centrifugation was performed to remove the debris after ultrasonication. Total protein was quantified in aliquots of cell lysate by using the bicinchoninic acid method (Pierce, Rockford, IL) and then used for determining the concentrations of HCV core Ag.

Figure 1A shows comparable levels of core Ag in each sample of cell lysate, as determined by immunoblotting with anti-FLAG antibody (Ab). The ability of HCV core Ag assays to detect five different HCV genotypes were compared using a commercially available chemiluminescence enzyme immunoassay (CLEIA) (Lumipulse II HCV core assay [assay detection range, approximately 50 to 50,000 fmol/liter]; Fujirebio, Japan) (15) and enzyme-linked immunosorbent assay (ELISA) (Ortho HCV Ag ELISA test [assay detection range, approximately 44.4 to 3,600 fmol/liter]; Ortho-Clinical Diagnostics, Japan) (2) to detect HCV core Ag in cell lysate. As shown in Fig. 1B,

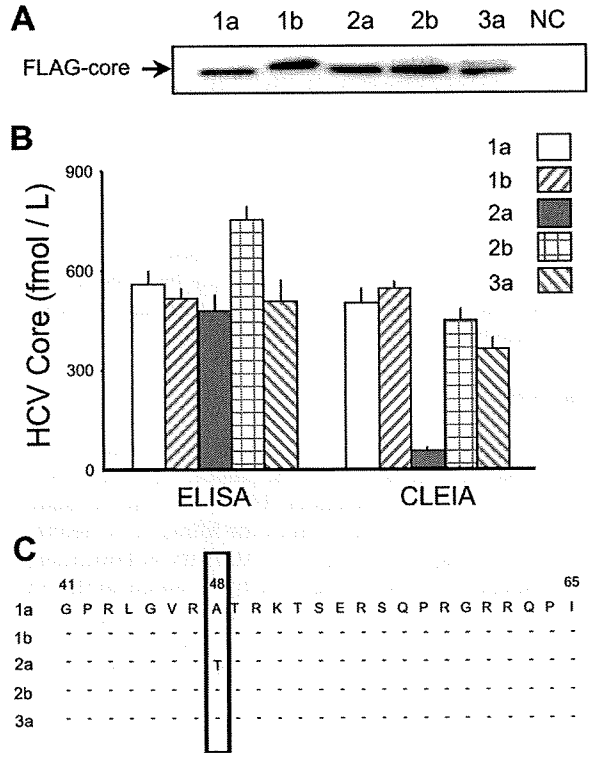

FIG. 1. Detection of recombinant HCV core Ag derived from genotype 1a, 1b, 2a, 2b, and 3a isolates by immunoblotting using an anti-FLAG Ab (A) as well as ELISA and CLEIA (B). The data shown in panel B represent the mean values and standard deviations (n = 3). NC, negative control. (C) The amino acid sequence from amino acids 41 to 65 of the core Ag used in this study. Key residues at the 48th position are boxed. Hyphens indicate conservation.

* Corresponding author. Mailing address: Department of Virology II, National Institute of Infectious Diseases, 1-23-1 Toyama, Shinjuku-ku, Tokyo 162-8640, Japan. Phone: 81-3-5285-1111. Fax: 81-3-5285-1161. E-mail: tesuzuki@nih.go.jp.

▽ Published ahead of print on 7 October 2009.

TABLE 1. Comparison of the 48th residues of HCV core Ags of genotypes 1a, 1b, 2a, 2b, and 3a

Genotype	No. of isolates	No. (%) of isolates with residue at 48th position		
		T	A	Other
1a	263	9 (3.5)	254 (96.5)	0 (0)
1b	298	2 (0.7)	294 (98.6)	2 (0.7)
2a	17	5 (29.5)	12 (70.5)	0 (0)
2b	17	0 (0)	17 (100)	0 (0)
3a	23	0 (0)	23 (100)	0 (0)
Total	618	16 (2.6)	600 (97.1)	2 (0.3)

although the ELISA measured similar concentrations of core Ag in all samples, apparent low levels of the genotype 2a core Ag, originally from an isolate known as the JFH-1 isolate (7), were detected using the CLEIA method, suggesting that some differences in the amino acid sequences corresponding to particular HCV genotypes or isolates may influence the sensitivity of core Ag detection. A comparison of the core Ag sequences, including the monoclonal Ab epitopes used in the development of CLEIA, revealed conservation of alanine at the 48th position in four clones, of genotypes 1a, 1b, 2b, and 3a, but not genotype 2a, for which there is a threonine at this position (Fig. 1C). Based on our analysis of sequences available from the HCV database (http://hcv.lanl.gov/content/sequence/NEWALIGN/align.html), alanine is highly conserved at the 48th residue of the core Ag for HCV isolates of genotypes 1a, 1b, 2b, and 3a (Table 1). In contrast, alanine and threonine occur in this position in 70.5% and 29.5%, respectively, of genotype 2a isolates. To examine whether the low sensitivity of the CLEIA method might be due to this particular amino acid change, we next replaced threonine with alanine at the 48th position of the JFH-1 core Ag (for

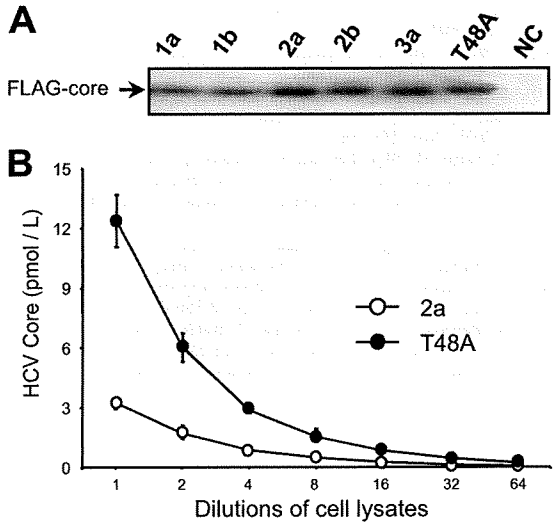

FIG. 2. Effect of T48A substitution in the core Ag of the JFH-1 isolate with regard to sensitivity of the CLEIA method. Samples of wild-type or mutated core Ag cell lysate were analyzed by immunoblotting (A) and CLEIA (B). The data shown in panel B represent the mean values and standard deviations (n = 3). NC, negative control.

TABLE 2. Comparison of the modified CLEIA with the original version for detection of the core Ags of genotypes 1a, 1b, 2a, 2b, and 3a[a]

Genotype	CLEIA	HCV core antigen concn (fmol/liter) in serially diluted cell lysates at indicated fold dilution							
		1	2	4	8	16	32	64	128
1a	Original	11,147	5,527	2,611	1,484	691	403	195	101
	Modified	10,511	5,700	2,676	1,420	716	444	200	111
1b	Original	11,612	5,618	3,081	1,551	779	409	223	113
	Modified	11,192	6,028	2,824	1,522	804	431	197	101
2a	Original	3,216	1,710	844	480	232	104	48	36
	Modified	12,101	6,255	3,153	1,676	805	422	212	106
2b	Original	10,559	5,635	2,811	1,286	762	387	194	94
	Modified	10,977	6,179	3,381	1,624	842	437	219	129
3a	Original	11,478	5,891	2,922	1,414	756	422	212	112
	Modified	11,208	6,225	3,126	1,555	791	445	215	100

[a] Data represent the mean values in triplicate measurements.

the mutant JFH-1coreT48A) and measured the HCV core Ag concentration in cells expressing both mutated and wild-type JFH-1 core Ag. After confirming comparable levels of FLAG-tagged core Ag in the cell lysate samples by immunoblotting (Fig. 2A), HCV core Ag was quantified in the samples by serial dilution via the CLEIA method. As shown in Fig. 2B, the core Ag concentrations of JFH-1coreT48A were assessed to be 3.2- to 3.8-fold higher than those of the wild-type core Ag, suggesting that the sensitivity of HCV core Ag detection may have been affected by the 48th residue in the core Ag. Data for samples derived from genotypes 1a, 1b, 2b, and 3a were analogous to data for JFH-1coreT48A (data not shown). Although HCV isolates with threonine at the 48th position of the core Ag sequence comprise a relatively small proportion of the major genotype population, only 2.6% of the genotype 1a, 1b, 2a, 2b, and 3a isolates here (16 of 618 isolates; Table 1), attempts to overcome this problem would improve the overall sensitivity and usefulness of the assay. To achieve this aim, another monoclonal anticore Ab, whose epitope is comprised of amino acids 50 to 65, which are completely conserved among all the genotypes examined (Fig. 1C), was therefore used as a second Ab in a modified version of the CLEIA. We compared this modified assay with the original version by measurement of core Ag concentrations of the various genotypes (Fig. 2A) as illustrated in Table 2. The modified assay was able to quantify core Ag from genotypes 1a, 1b, 2a, 2b, and 3a with no significant differences observed between Ag levels in samples from different genotypes at each dilution.

It has been demonstrated that the HCV core Ag assay is a useful alternative to HCV RNA quantification for the diagnosis of hepatitis C and for monitoring the antiviral effects of treatment. Compared to various reverse transcription-PCR methods, HCV core assays are less expensive and easier to perform, without the requirement of sophisticated laboratory equipment and specially trained laboratory personnel. In addition, the core Ag assay can be used to measure a more diverse set of blood samples, such as sera stored for a long period of time, because the viral Ag is generally more stable than the RNA in sera or plasma. Despite the adequate performance of core Ag assays, we have shown that a single amino acid substitution at the 48th position of the core Ag changes the detection sensitivity. It is also noted that, although the original CLEIA should be improved, the ELISA used in this study may be substituted for it.

In conclusion, we have identified a distinct anticore Ab with a different epitope that might enable improved detection across all of the major HCV isolates. The findings of this study would provide useful information for the development of an improved assay with greater accuracy.

We thank Ortho-Clinical Diagnostics K.K. and Fujirebio Inc. for providing the diagnostic kits and for helping us in performing the assays.

This work was supported by a grant-in-aid for scientific research from the Ministry of Health, Labor and Welfare of Japan.

REFERENCES

1. **Aizaki, H., Y. Aoki, T. Harada, K. Ishii, T. Suzuki, S. Nagamori, G. Toda, Y. Matsuura, and T. Miyamura.** 1998. Full-length complementary DNA of hepatitis C virus genome from an infectious blood sample. Hepatology **27:** 621–627.
2. **Aoyagi, K., C. Ohue, K. Iida, T. Kimura, E. Tanaka, K. Kiyosawa, and S. Yagi.** 1999. Development of a simple and highly sensitive enzyme immunoassay for hepatitis C virus core antigen. J. Clin. Microbiol. **37:**1802–1808.
3. **Bouvier-Alias, M., K. Patel, H. Dahari, S. Beaucourt, P. Larderie, L. Blatt, C. Hezode, G. Picchio, D. Dhumeaux, A. U. Neumann, J. G. McHutchison, and J. M. Pawlotsky.** 2002. Clinical utility of total HCV core antigen quantification: a new indirect marker of HCV replication. Hepatology **36:**211–218.
4. **Buti, M., C. Mendez, M. Schaper, S. Sauleda, A. Valdes, F. Rodriguez-Frias, R. Jardi, and R. Esteban.** 2004. Hepatitis C virus core antigen as a predictor of non-response in genotype 1 chronic hepatitis C patients treated with peginterferon alpha-2b plus ribavirin. J. Hepatol. **40:**527–532.
5. **Chevaliez, S., and J. M. Pawlotsky.** 2007. Practical use of hepatitis C virus kinetics monitoring in the treatment of chronic hepatitis C. J. Viral Hepat. **14** (Suppl. 1)**:**77–81.
6. **González, V., E. Padilla, M. Diago, M. D. Gimenez, R. Sola, L. Matas, S. Montoliu, R. M. Morillas, C. Perez, and R. Planas.** 2005. Clinical usefulness of total hepatitis C virus core antigen quantification to monitor the response to treatment with peginterferon alpha-2a plus ribavirin. J. Viral Hepat. **12:**481–487.
7. **Kato, T., A. Furusaka, M. Miyamoto, T. Date, K. Yasui, J. Hiramoto, K. Nagayama, T. Tanaka, and T. Wakita.** 2001. Sequence analysis of hepatitis C virus isolated from a fulminant hepatitis patient. J. Med. Virol. **64:**334–339.
8. **Laperche, S.** 2005. Blood safety and nucleic acid testing in Europe. Euro Surveill. **10:**3–4.
9. **Maynard, M., P. Pradat, P. Berthillon, G. Picchio, N. Voirin, M. Martinot, P. Marcellin, and C. Trepo.** 2003. Clinical relevance of total HCV core antigen testing for hepatitis C monitoring and for predicting patients' response to therapy. J. Viral Hepat. **10:**318–323.
10. **Netski, D. M., X. H. Wang, S. H. Mehta, K. Nelson, D. Celentano, S. Thongsawat, N. Maneekarn, V. Suriyanon, J. Jittiwutikorn, D. L. Thomas, and J. R. Ticehurst.** 2004. Hepatitis C virus (HCV) core antigen assay to detect ongoing HCV infection in Thai injection drug users. J. Clin. Microbiol. **42:**1631–1636.
11. **Niwa, H., K. Yamamura, and J. Miyazaki.** 1991. Efficient selection for high-expression transfectants with a novel eukaryotic vector. Gene **108:**193–199.
12. **Nübling, C. M., G. Unger, M. Chudy, S. Raia, and J. Lower.** 2002. Sensitivity of HCV core antigen and HCV RNA detection in the early infection phase. Transfusion **42:**1037–1045.
13. **Roth, W. K., M. Weber, and E. Seifried.** 1999. Feasibility and efficacy of routine PCR screening of blood donations for hepatitis C virus, hepatitis B virus, and HIV-1 in a blood-bank setting. Lancet **353:**359–363.
14. **Suzuki, T., K. Ishii, H. Aizaki, and T. Wakita.** 2007. Hepatitis C viral life cycle. Adv. Drug Deliv. Rev. **59:**1200–1212.
15. **Takahashi, M., H. Saito, M. Higashimoto, K. Atsukawa, and H. Ishii.** 2005. Benefit of hepatitis C virus core antigen assay in prediction of therapeutic response to interferon and ribavirin combination therapy. J. Clin. Microbiol. **43:**186–191.
16. **Tanaka, E., C. Ohue, K. Aoyagi, K. Yamaguchi, S. Yagi, K. Kiyosawa, and H. J. Alter.** 2000. Evaluation of a new enzyme immunoassay for hepatitis C virus (HCV) core antigen with clinical sensitivity approximating that of genomic amplification of HCV RNA. Hepatology **32:**388–393.
17. **Yanagi, M., R. H. Purcell, S. U. Emerson, and J. Bukh.** 1999. Hepatitis C virus: an infectious molecular clone of a second major genotype (2a) and lack of viability of intertypic 1a and 2a chimeras. Virology **262:**250–263.

Antiviral Research 83 (2009) 112–117

Contents lists available at ScienceDirect

Antiviral Research

journal homepage: www.elsevier.com/locate/antiviral

Identification of bisindolylmaleimides and indolocarbazoles as inhibitors of HCV replication by tube-capture-RT-PCR

Yuko Murakami[a,*], Kohji Noguchi[a], Satoshi Yamagoe[a], Tetsuro Suzuki[b], Takaji Wakita[b], Hidesuke Fukazawa[a,*]

[a] Department of Bioactive Molecules, National Institute of Infectious Diseases, Toyama 1-23-1, Shinjuku-ku, Tokyo 162-8640, Japan
[b] Department of Virology II, National Institute of Infectious Diseases, Tokyo, Japan

ARTICLE INFO

Article history:
Received 31 July 2008
Received in revised form 10 February 2009
Accepted 27 March 2009

Keywords:
HCV
Bisindolylmaleimide
Tube-capture-RT-PCR
High-throughput

ABSTRACT

We devised a screening method for hepatitis C virus (HCV) inhibitors by exploiting the JFH1 viral culture system. The viral RNA released in the medium was adsorbed onto PCR plates, and real-time RT-PCR was performed by directly adding the one-step RT-PCR reaction mixture to the wells. The "tube-capture-RT-PCR" method obviates the need for labor-intensive RNA isolation and should allow high-throughput screening of HCV inhibitors. To substantiate the validity of the assay for drug screening, a pilot screen of an inhibitor library composed of 95 compounds was performed. In addition to the known inhibitors of HCV replication included in the library, the assay identified the PKC inhibitor bisindolylmaleimide I (BIM I) as an HCV replication inhibitor. BIM I was also effective in reducing the viral protein level in genotype 1b and 2a subgenomic replicon cells, indicating inhibition of HCV replication. Further assays revealed that a broad range of bisindolylmaleimides and indolocarbazoles inhibit HCV, but no correlation was found between the PKC inhibition pattern and anti-HCV activity. These series of compounds represent new classes of inhibitors that may warrant further development.

1. Introduction

Hepatitis C virus, a major cause of chronic liver disease, has infected over 170 million people. The current mainstream anti-HCV therapy is a combination of interferon (IFN) and ribavirin. However, the therapy is not effective in approximately half of HCV-infected patients and has considerable side effects in many patients; thus, there is an urgent need for novel HCV therapies.

Various assays for HCV drug screening have been reported, many of which rely on HCV replicon systems. Although HCV replicon-based systems have greatly facilitated HCV research and drug discovery, these systems do not completely reflect the entire HCV life cycle and are not capable of identifying inhibitors of several important steps such as viral attachment, entry, and release. The recently introduced HCV cell culture systems (Wakita et al., 2005) should overcome these limitations and enable identification of inhibitors that would not be recognized by the replicon-based screens.

Here we describe a simple screening method for discovering anti-HCV drugs using the JFH1 viral culture system. Antiviral activity was determined by RT-PCR measurement of viral RNA released in the medium of infected cells. To increase efficiency, we devised a method that avoids tedious RNA isolation.

As a proof of concept, the method was used to evaluate a compound library and successfully confirmed the anti-HCV activity of cyclosporin A. In addition, a potent and selective PKC inhibitor, BIM I, was also identified as an anti-HCV agent. We found that other bisindolylmaleimides and indolocarbazoles also inhibit HCV, whereas anti-HCV activity was not associated with PKC inhibition. HCV inhibition by bisindolylmaleimides or indolocarbazoles has not been reported, and we expect that our assay will facilitate the identification of previously unrecognized HCV inhibitors. The bisindolylmaleimides and indolocarbazoles are already in clinical trials and may merit attention as HCV drug candidates.

2. Materials and methods

2.1. Cells and virus

Plasmid pJFH1, containing full-length cDNA of the JFH1 isolate, was used to generate HCV production in cell culture, as described elsewhere (Wakita et al., 2005), and the supernatant was passaged in Huh 7.5.1 cells. To prepare virus stock for screening, naïve Huh 7.5.1 cells were infected with the passaged supernatant virus, and the medium was collected 7 days post-infection and stored at

* Corresponding authors. Tel.: +81 3 5285 1111x2327; fax: +81 3 5285 1272.
E-mail addresses: murakami@nih.go.jp (Y. Murakami), fukazawa@nih.go.jp (H. Fukazawa).

0166-3542/$ – see front matter © 2009 Elsevier B.V. All rights reserved.
doi:10.1016/j.antiviral.2009.03.008

–80 °C until use. The infectious titers of the viruses were determined by immunofluorescence analysis of the infected Huh 7.5.1 cells using anti-core antibody (2H9). The infectious titers of the stocks were generally about 3×10^5–1×10^6 ffu/ml, corresponding to about 3×10^7–1×10^8 copies of JFH1 RNA/ml. A subgenomic replicon cell, clone 4-1, which harbors the genotype 2a HCV genome (Kato et al., 2003; Date et al., 2004) and clone 5-15, which harbors the genotype 1b HCV genome (Lohmann et al., 1999), were also cultured in Dulbecco's Modified Eagle's medium (DMEM) with fetal bovine serum (FBS).

2.2. Reagents

The SCADS inhibitor kit I was provided by the Screening Committee of Anticancer Drugs supported by a Grant-in-Aid for Scientific Research on the Priority Area "Cancer" from The Ministry of Education, Culture, Sports, Science and Technology, Japan. The PKC β isozyme selective inhibitor LY333531 (Ruboxistaurin) was from Alexis Corp. (Lausen, Switzerland). Other chemicals were purchased from Merck Calbiochem (Darmstadt, Germany). Interferon-α (IFN-α) was from PeproTech, Inc. (Princeton Business Park, Princeton, NJ).

2.3. Quantitative real-time RT-PCR

Huh 7.5.1. cells were seeded in 96-well plates at a density of 20,000 cells per well in a volume of 120 μl. The next day, 15 μl of test compounds was added and the cells were infected with 15 μl of virus stock of HCV-JFH1 at a multiplicity of infection (MOI) of 0.01. After 5 days of culture, 100 μl of medium was transferred to a PCR plate, incubated on ice for 30 min, centrifuged at 3500 rpm for 15 min, and then removed. Twenty microliters of One Step SYBR PrimeScript RT-PCR Kit reaction mixture (Takara-Bio Co., Otsu, Japan) was added into the PCR plate wells, and quantitative real-time PCR was performed using an ABI Prism 7000 sequence detector (PE Applied Biosystems, Foster City, CA). The primers used were 5′-GAGTGTCGTACAGCCTCCAG-3′ (nucleotides 97–116), and 5′-AGGCCTTTCGCAACCCA-3′ (nucleotides 280–264) from the noncoding region of HCV-JFH1, at a concentration of 200 nM. Media from the control wells without drug were serially diluted to create a standard curve, which was used to determine the relative amount of HCV RNA in the media of HCV-infected cells treated with the compounds. Cell growth was monitored by MTT assay, as described previously (Fukazawa et al., 1995).

For further analysis of the drug effect and determination of the copy number of HCV RNA in medium and cells, HCV RNA was extracted from 140 μl medium with the QIAamp Viral RNA mini kit (QIAGEN GmbH, Hilden, Germany), and eluted with 60 μl of elution buffer. Eight microliters of the viral RNA eluate was subjected to quantitative real-time PCR using Taqman EZ RT-PCR Core reagents (PE Applied Biosystems). The primers were 5′-CGGGAGAGCCATAGTGG (nucleotides 129–145) and 5′-AGTACCACAAGGCCTTTCG (nucleotides 289–271) at a concentration of 200 nM, and the Taqman probe was FAM-5′-CTGCGGAACCGGTGAGTACAC-3′-TAMRA (nucleotides 147–167) at a concentration of 300 nM (Takeuchi et al., 1999). Standard JFH1 RNA for measurement of copy number was transcribed from plasmid pSRG-JFH1-Luci, which was derived from pSRG-JFH1 (Kato et al., 2003), using the AmpliScribe T7 High Yield Transcription Kit (Epicentre Biotechnologies, Madison, WI). The transcribed RNA was purified and diluted with ribonuclease-free water containing yeast tRNA and 0.2% DTT, as previously described (Suzuki et al., 2005).

2.4. Western blotting

Cells were lysed with Radio-ImmunoPrecipitation Assay (RIPA) buffer (50 mM Tris–HCl, pH 8.0, 150 mM NaCl, 0.1% SDS, 0.5% sodium deoxycholate, 1% NP-40, 1 mM EDTA) containing 1 mM phenylmethylsulfonyl fluoride (PMSF) and 25 μg/ml of each of antipain, pepstatin, and leupeptin, and centrifuged. The amount of protein in the supernatant was then measured. Cell lysates containing equal amounts of protein were separated by SDS-PAGE, transferred onto polyvinylidene difluoride (PVDF) membranes, and probed with antibodies against core (2H9), NS5A (Austral Biologicals, San Raman, CA), α-tubulin (Merck Calbiochem), and GAPDH (Santa Cruz Biotech. Inc., Santa Cruz, CA). The membranes were incubated with horseradish peroxidase-conjugated secondary antibodies and specific proteins were visualized by chemiluminescence.

3. Results

3.1. Assay development

To establish an efficient RT-PCR-based screen for anti-HCV agents, we searched for methods that could be carried out without labor-intensive RNA isolation. We tested whether tube-trapping methods used to obtain plant viral RNAs for RT-PCR (Rowhani et al., 1995; James, 1999; Suehiro et al., 2005) could be applied to HCV. A JFH1 stock solution (3×10^5 ffu/ml, 3×10^7 copies/ml) was serially diluted fourfold, put into the wells of the PCR plate, incubated on ice for 30 min, and then centrifuged at 3500 rpm for 15 min. The supernatant was removed and quantitative RT-PCR was performed by direct addition of the one-step RT-PCR reaction mixture. We found that HCV, like plant viruses, are adsorbed onto the well wall during incubation. As shown in Fig. 1a, RNA adsorption appeared to be linear over a broad range of viral concentrations. HCV RNA could still be detected after seven fourfold dilutions, indicating that the "tube-capture" is a quantitative method that can detect less than 200 copies of HCV RNA. We compared the CT values from this "tube-capture method" with those from the conventional method of RNA extraction. The efficiency of RNA recovery by "tube-capture" was calculated to be about 9% of the conventional method. However, as shown in Fig. 1a, there was a close correlation between the CT values obtained from the two methods ($R = 0.988$), demonstrating the usefulness of this method.

3.2. Identification of BIM I as an inhibitor of HCV infection

To explore the possibility of tube-capture-RT-PCR as a simple screen for discovering anti-HCV compounds, we first tested whether the method would detect the antiviral activity of IFN-α. Huh7.5.1 cells were seeded in a 96-well plate and infected with HCV-JFH1 at an MOI of 0.01. After 5 days, HCV RNA released in the medium was assayed by the tube-capture method. Under these conditions, the CT from the control medium was usually about 18–20. As shown in Fig. 1b, a substantial reduction in the amount of HCV RNA was observed when the cells were infected in the presence of IFN-α.

For further validation of the ability of the assay to identify HCV inhibitors, we performed a pilot screen using an inhibitor kit provided by the Screening Committee of Anticancer Drugs (SCADS inhibitor kit I). This kit contains 95 inhibitors including cyclosporin A, a compound reported to inhibit HCV replication.

Cyclosporin A was identified (Fig. 1c), providing a proof of concept for screening for anti-HCV drug candidates. In addition, our assay also identified the PKC inhibitor bisindolylmaleimide I (BIM I) (Fig. 2a, black columns). The IC_{50} was about 0.1 μM, which is comparable to that of cyclosporin A and about 200-fold lower than the IC_{50} for cell growth (Fig. 2b). In addition, BIM I inhibited the cytopathic effect of HCV JFH1. Infection with HCV resulted in about a 20% reduction of cell growth. BIM I at 1 μM enhanced the growth of

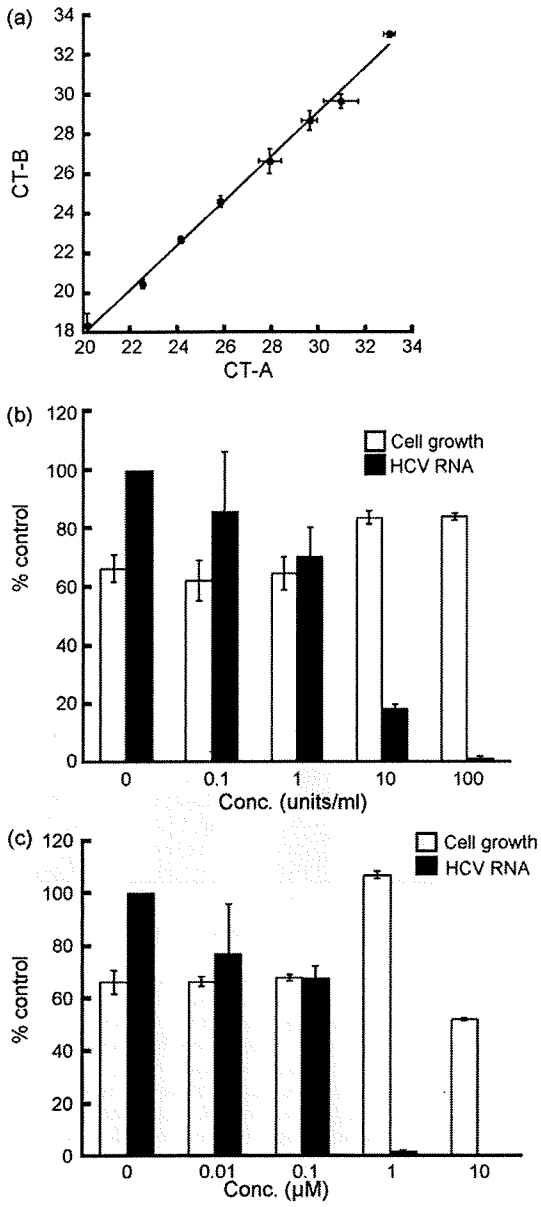

Fig. 1. RT-PCR-based screen for anti-HCV agents using the JFH1 viral culture system. (a) Correlation between CT values from "tube-capture-RT-PCR" (CT-A) and ordinary RNA extraction (CT-B). JFH1 stock solution (3×10^5 ffu/ml) was serially diluted four-fold and quantitative real-time PCR was performed as described under Section 2. CT-A was the average CT of three wells using tube-capture-RT-PCR and CT-B was the average CT of three HCV RNA eluates using a kit (QIAamp Viral RNA mini). (b) and (c) Huh 7.5.1 cells were infected with JFH1 in the presence of the indicated concentrations of IFN-α (b) or cyclosporin A (c). HCV RNA in the medium (closed (black) columns) was assessed by "tube-capture-RT-PCR" as described under Section 2. Open (white) columns represent percentage of cell growth compared with that of control cells without virus and compound. Columns, mean of triplicate wells; bars, SD.

infected cells, almost to the level of uninfected cells (Fig. 2a, white columns). Recovery of cell growth was also observed with INF-α or cyclosporin A treatment (Fig. 1b and c). BIM I reduced cell growth of uninfected cells only at concentrations of 1 μM or higher (Fig. 2b). BIM I also inhibited the production of the HCV core protein with marginal effects on host α-tubulin levels (Fig. 2c).

3.3. BIM I inhibits HCV replication

To our knowledge, the anti-HCV effects of BIM I or other PKC inhibitors have not been reported. Because the majority of current

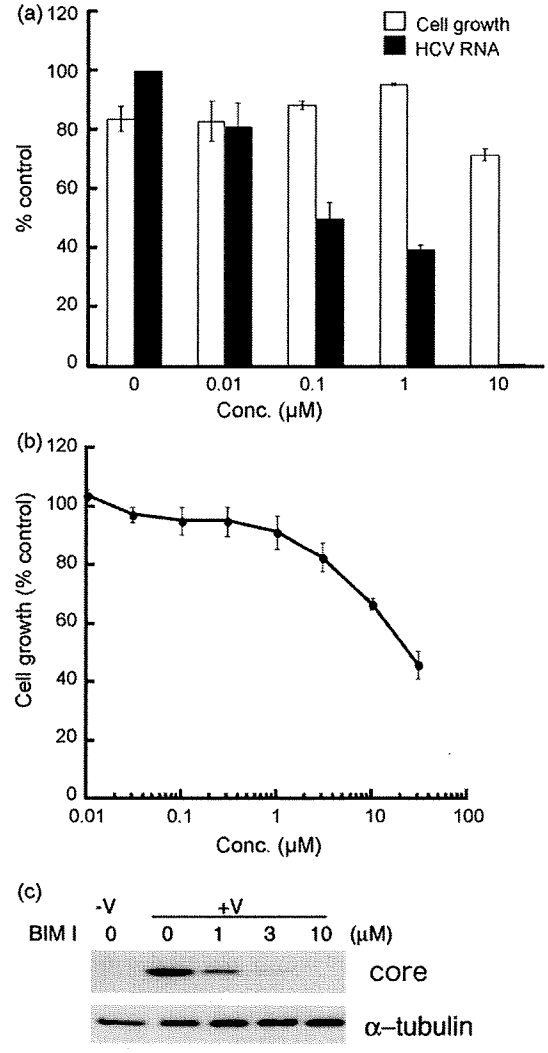

Fig. 2. BIM I inhibits HCV. (a) Effects of BIM I on HCV JFH1 RNA. Huh 7.5.1 cells were infected with JFH1 in the presence of the indicated concentrations of BIM I and assayed for HCV RNA and cell growth as in Fig. 1. Columns, mean of triplicate wells; bars, SD. (b) Effects of BIM I on growth of Huh 7.5.1 cells. (c) Effects of BIM I on HCV core protein in cells. Cells were infected with JFH1 at an MOI of 0.2 in the presence of the indicated concentrations of BIM I and cultured for 2 days. Cells were lysed and subjected to western blotting as described under Section 2. "V" indicates infection with HCV.

HCV drug screening relies on replicon-based models, we investigated the possibility that BIM I targets a step in the HCV life cycle that is not included in the replicon systems, such as attachment, entry or release. We treated two subgenomic replicon cells with BIM I and examined the amount of NS5A protein.

As shown in Fig. 3a and b, BIM I dose-dependently reduced NS5A in both 1b and 2a subgenomic replicon cells, but not the host GAPDH. The results indicate that BIM I inhibits a process involved in the replication of HCV subgenomic replicons. However, although the NS5A level appeared to be more vulnerable, cell growth was substantially suppressed by BIM I (Fig. 3c). Whereas a significant difference between the IC_{50} for HCV RNA and cell growth was observed in the HCV cell culture system, the reduction of NS5A in replicon cells overlapped with the effects on cell growth.

To further elucidate the stage of the HCV life cycle affected by BIM I, Huh 7.5.1 cells were inoculated with higher titers of JFH1 (MOI 2) and then treated with 3 μM BIM I, starting at different time points after infection. JFH1 appeared to complete the life cycle in about 48 h, judging from the expression profiles of viral RNA and proteins in cells (Fig. 4a). When BIM I was added at the time of infection,

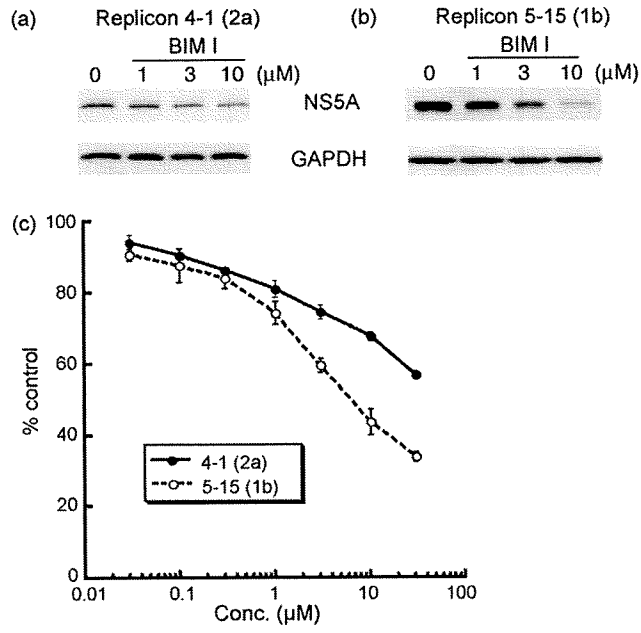

Fig. 3. Effect of BIM I on subgenomic replicon cells. (a) Subgenomic replicon cells harboring genotype 2a (4-1) (a) and genotype 1b (5-15) (b) were treated with BIM I for 2 or 4 days, respectively. Cells were lysed and analyzed by western blotting with anti-NS5A antibody or anti-GAPDH antibody. (c) Effect of BIM I on cell growth of the two replicon cells. Cells were incubated for 2 (4-1) or 4 days (5-15) with BIM I, and cell growth was measured by MTT assay.

the amount of viral RNA in the medium after 48 h decreased to less than 20% of control cells without inhibitor treatment. Addition of BIM I at 6 h post-infection still resulted in a reduction of viral RNA to 30% of control, but after 24 h the antiviral activity of BIM I was significantly diminished and only a modest decline to about 80% was observed (Fig. 4b). These results suggest that interference with RNA synthesis or translation of viral proteins accounts, at least in part, for the anti-HCV activity of BIM I.

3.4. *HCV inhibition by bisindolylmaleimide and indolocarbazole compounds does not involve PKC*

Since the discovery of staurosporine as a broad-spectrum protein kinase inhibitor, a variety of bisindolylmaleimide and indolocarbazole inhibitors with different potencies and selectivity have been developed. BIM I is one such compound that is highly specific for PKC and is broadly used to analyze PKC-mediated events. To gain insight into the relevance of the PKC inhibitory spectrum and antiviral activity, panels of different bisindolylmaleimide and indolocarbazole compounds were tested in the assays. Contrary to our expectation, no correlation was found between the ability to inhibit PKC and HCV.

Another bisindolylmaleimide PKC inhibitor without the N-dimethylaminopropyl chain, BIM IV, displayed similar significant anti-HCV activity (Fig. 5). Other structurally related pan- and isozyme-specific PKC inhibitors such as BIM II, Ro31-8220 (BIM IX), LY333,531 and 3-(1-(3-imidazol-1-ylpropyl)-1H-indol-3-yl)-4-anilino-1H-pyrrole-2,5-dione (PKCβ Inhibitor, Calbiochem) or an indolocarbazole compound K252c also inhibited HCV replication (not shown). However, as shown in Fig. 5, the non-PKC-inhibitory analog BIM V (Toullec et al., 1991) and arcyriaflavin A, an indolocarbazole compound with no reported effects on PKC (Zhu et al., 2003), were also effective in reducing HCV RNA. BIM V was actually more potent than BIM I. Whereas the effect of BIM I on HCV overlapped with cytotoxicity in this particular experiment, BIM V was virtually nontoxic at a dose (1 μM) that reduced

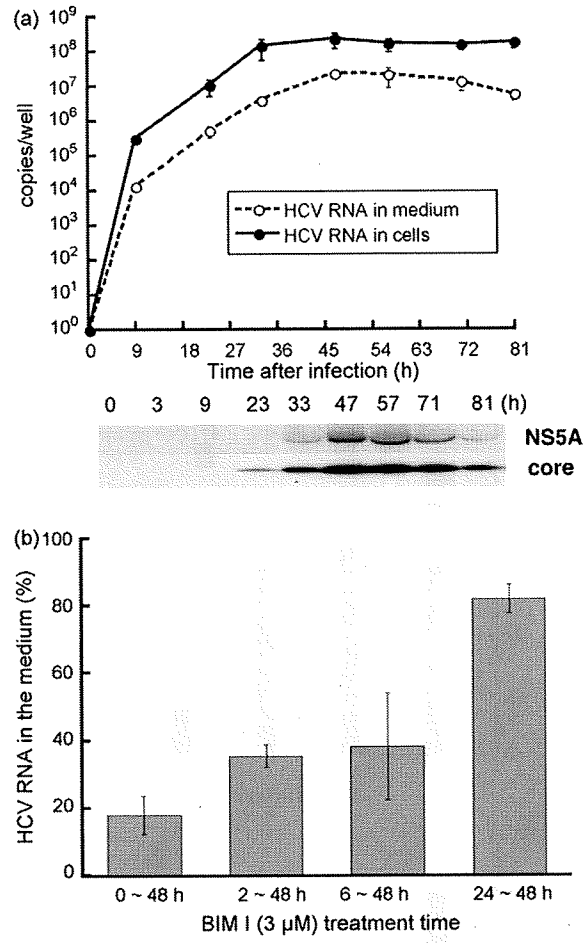

Fig. 4. (a) Expression profile of the HCV RNA and proteins. Huh 7.5.1 cells were infected with HCV as described above, but at an MOI of 2. The cells and medium were harvested at the indicated time and analyzed for HCV RNA and proteins. The core and NS5A protein were detected in the cell lysate. (b) Effect of time of addition. BIM I (3 μM) was added to Huh 7.5.1 cells just before and 2, 6, or 24 h after HCV addition at an MOI of 0.2. After 48 h of incubation following virus infection, the HCV RNA in the medium was extracted and measured with quantitative real-time RT-PCR. The indicated values represent the averages for two independent experiments.

HCV RNA to less than 20% of control. The results indicate that a broad range of bisindolylmaleimide and indolocarbazole compounds inhibit HCV replication, albeit in a PKC-independent manner.

4. Discussion

HCV replicon systems have made significant contributions in HCV research and drug development. Nevertheless, as drug screening tools, replicon systems have limitations because they are not capable of identifying inhibitors of several important events in the viral life cycle. The use of HCV cell culture systems should overcome the drawbacks of the replicon systems and facilitate the identification of inhibitors with novel mechanisms of action. Actually, it has recently been shown that use of an infectious HCV system identified inhibitors that a replicon-based screen did not recognize (Zhang et al., 2008).

We developed a simple screening method for HCV inhibitors that measures the viral RNA released from JFH1-infected cells. The assay does not require specially engineered viruses. The "tube-capture-RT-PCR" method obviates the need for labor-intensive RNA isolation and significantly increases the efficiency of screening. The validity of the assay was confirmed by successful identification of known

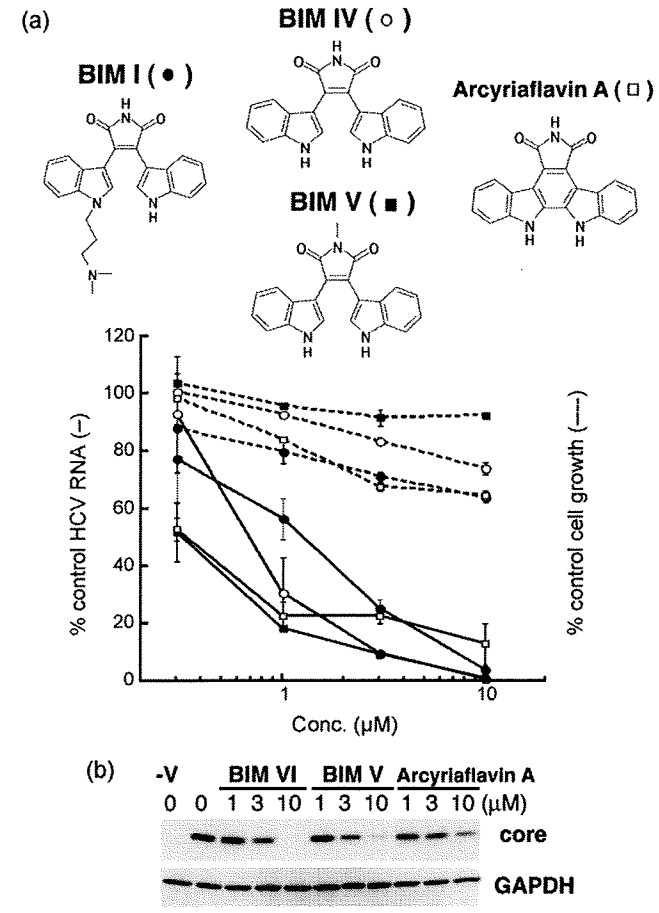

Fig. 5. Effects of bisindolylmaleimide or indolocarbazole compounds on HCV infection. (a) Effects of BIM I, BIM IV, BIM V, and arcyriaflavin A on HCV RNA in the medium. Huh 7.5.1 cells were seeded and infected with HCV at an MOI of 0.01 in the presence of drugs. After 4 days of incubation, the HCV RNA in the medium was extracted and quantified. The relative amounts of HCV RNA with BIM I (closed circle), BIM IV (open circle), BIM V (closed rectangle), and arcyriaflavin A (open rectangle) are represented by solid lines. Cell viability, represented by dotted lines, was determined by MTT assay of a parallel culture without HCV challenge. (b) Effects of BIM IV, BIM V and arcyriaflavin A on core proteins in cells. The cells were infected with JFH1 at an MOI of 0.2 in the presence of the indicated concentrations of compounds and analyzed as described in Fig. 2c. "–V" indicates control without HCV infection.

HCV inhibitors in the pilot screen. In addition, the assay identified the PKC inhibitor BIM I.

BIM I is a widely used compound, and it was somewhat surprising to us that its anti-HCV activity had not been reported. HCV replication in the cell culture system appeared to be considerably more susceptible to BIM I than in the replicon systems, and this is probably why this compound had not been identified as an HCV inhibitor.

Because virus replication is closely linked to host cell growth, HCV inhibition could occur as a result of cell growth inhibition. However, as shown in Fig. 2a, BIM I reduced the cytopathic effect of HCV infection just like interferon-α and cyclosporin A. BIM I, at 1 μM, enhanced the growth of infected cells almost to the level of uninfected cells, presumably because HCV replication, but not cell growth, was inhibited, resulting in a reversal of the cytopathic effect.

Because the PKC inhibitory properties of bisindolylmaleimides and indolocarbazoles have been characterized extensively, we tested a panel of commercially available compounds in the assay to gain insight into the role of PKC in HCV replication. However, no correlation between PKC inhibition and antiviral activity could be found. Anti-HCV activity did not involve PKC inhibition, apparently because a non-PKC-inhibitory analog, BIM V, was also active. Furthermore, PKC inhibitors with different structures, such as calphostin C and H-7, did not show specific inhibition of HCV (data not shown).

Previous studies have indicated that bisindolylmaleimide PKC inhibitors have cellular targets other than PKC. It has been shown that BIM I and Ro31-8220 inhibit p70S6K and p90RSK (Alessi, 1997; Roberts et al., 2005) and that BIM V inhibits p70S6K (Marmy-Conus et al., 2002). Although we did not monitor the activities of these enzymes in our experiments, inhibition of p70S6K is unlikely to be responsible for the anti-HCV effect of PKC inhibitors, because Ishida et al. reported that silencing of p70S6K enhanced HCV RNA abundance (Ishida et al., 2007).

Bisindolylmaleimides and indolocarbazoles have also been reported to inhibit the ATP-binding cassette (ABC) transporters P-glycoprotein and multidrug resistance-associated protein 1 (MRP1), efflux pumps that play important roles in cancer drug resistance (Merritt et al., 1999; Gekeler et al., 1995). More recently, Robey et al. reported that BIMs I, II, III, IV, and V, K252c, and arcyriaflavin A inhibit ABCG2, an ABC half-transporter that confers resistance to various antitumor agents (Robey et al., 2007). Whether ABC transporters play any role in HCV infection awaits further study. We are currently examining the anti-HCV effects of other ABC transporter inhibitors.

In conclusion, we developed a simple infectious HCV system-based assay that can be used for high-throughput screening of HCV inhibitors and identified bisindolylmaleimides and indolocarbazoles. These compounds might represent lead substances for the development of new HCV drugs. Further analysis of the mechanism of HCV-inhibition by these compounds might reveal a new mechanism of regulation of HCV infection.

Acknowledgments

We thank Drs. Kyoko Murakami, Kenichi Morikawa and Tomoko Date for helpful advice. This study was supported by a grant-in-Aid from the Ministry of Health, Labor and Welfare of Japan.

References

Alessi, D.R., 1997. The protein kinase C inhibitors Ro 318220 and GF 109203X are equally potent inhibitors of MAPKAP kinase-1β (Rsk-2) and p70 S6 kinase. FEBS Lett. 402, 121–123.

Date, T., Kato, T., Miyamoto, M., Zhao, Z., Yasui, K., Mizokami, M., Wakita, T., 2004. Genotype 2a hepatitis C virus subgenomic replicon can replicate in HepG2 and IMY-N9 cells. J. Biol. Chem. 279, 22371–22376.

Fukazawa, H., Mizuno, S., Uehara, Y., 1995. A microplate assay for quantitation of anchorage-independent growth of transformed cells. Anal. Biochem. 228, 83–90.

Gekeler, V., Boer, R., Ise, W., Sanders, K.H., Schächtele, C., Beck, J., 1995. The specific bisindolylmaleimide PKC-inhibitor GF 109203X efficiently modulates MRP-associated multiple drug resistance. Biochem. Biophys. Res. Commun. 206, 119–126.

Ishida, H., Li, K., Yi, M., Lemon, S.M., 2007. p21-activated kinase 1 is activated through the mammalian target of rapamycin/p70 S6 kinase pathway and regulates the replication of hepatitis C virus in human hepatoma cells. J. Biol. Chem. 282, 11836–11848.

James, D., 1999. A simple and reliable protocol for the detection of apple stem grooving virus by RT-PCR and in a multiplex PCR assay. J. Virol. Methods 83, 1–9.

Kato, T., Date, T., Miyamoto, M., Furusaka, A., Tokushige, K., Mizokami, M., Wakita, T., 2003. Efficient replication of the genotype 2a hepatitis C virus subgenomic replicon. Gastroenterology 125, 1808–1817.

Lohmann, V., Körner, F., Koch, J., Herian, U., Theilmann, L., Bartenschlager, R., 1999. Replication of subgenomic hepatitis C virus RNAs in a hepatoma cell line. Science 285, 110–113.

Marmy-Conus, N., Hannan, K.M., Pearson, R.B., 2002. Ro 31-6045, the inactive analogue of the protein kinase C inhibitor Ro 31-8220, blocks in vivo activation of p70(s6k)/p85(s6k): implications for the analysis of S6K signalling. FEBS Lett. 519, 135–140.

Merritt, J.E., Sullivan, J.A., Drew, L., Khan, A., Wilson, K., Mulqueen, M., Harris, W., Bradshaw, D., Hill, C.H., Rumsby, M., Warr, R., 1999. The bisindolylmaleimide protein kinase C inhibitor, Ro 32-2241, reverses multidrug resistance in KB tumour cells. Cancer Chemother. Pharmacol. 43, 371–378.

Roberts, N.A., Haworth, R.S., Avkiran, M., 2005. Effects of bisindolylmaleimide PKC inhibitors on p90RSK activity in vitro and in adult ventricular myocytes. Br. J. Pharmacol. 145, 477–489.

Robey, R.W., Shukla, S., Steadman, K., Obrzut, T., Finley, E.M., Ambudkar, S.V., Bates, S.E., 2007. Inhibition of ABCG2-mediated transport by protein kinase inhibitors with a bisindolylmaleimide or indolocarbazole structure. Mol. Cancer Ther. 6, 1877–1885.

Rowhani, A., Maningas, M.A., Lile, L.S., Daubert, S.D., Golino, D.A., 1995. Development of a detection system for viruses of woody plants based on analysis of immobilized virions. Phytopathology 85, 347–352.

Suehiro, N., Matsuda, K., Okuda, S., Natsuaki, T., 2005. A simplified method for obtaining plant viral RNA for RT-PCR. J. Virol. Methods 125, 67–73.

Suzuki, T., Omata, K., Satoh, T., Miyasaka, T., Arai, C., Maeda, M., Matsuno, T., Miyamura, T., 2005. Quantitative detection of hepatitis C virus (HCV) RNA in saliva and gingival crevicular fluid of HCV-infected patients. J. Clin. Microbiol. 43, 4413–4417.

Takeuchi, T., Katsume, A., Tanaka, T., Abe, A., Inoue, K., Tsukiyama-Kohara, K., Kawaguchi, R., Tanaka, S., Kohara, M., 1999. Real-time detection system for quantification of hepatitis C virus genome. Gastroenterology 116, 636–642.

Toullec, D., Pianetti, P., Coste, H., Bellevergue, P., Grand-Perret, T., Ajakane, M., Baudet, V., Boissin, P., Boursier, E., Loriolle, F., Duhamel, L., Charon, D., Kirilovsky, J., 1991. The bisindolylmaleimide GF 109203X is a potent and selective inhibitor of protein kinase C. J. Biol. Chem. 266, 15771–15781.

Wakita, T., Pietschmann, T., Kato, T., Date, T., Miyamoto, M., Zhao, Z., Murthy, K., Habermann, A., Kräusslich, H., Mizokami, M., Bartenschlager, R., Liang, T.J., 2005. Production of infectious hepatitis C virus in tissue culture from a cloned viral genome. Nat. Med. 11, 791–796.

Zhang, Y., Weady, P., Duggal, R., Hao, W., 2008. Novel chimeric genotype 1b/2a hepatitis C virus suitable for high-throughput screening. Antimicrob. Agents Chemother. 52, 666–674.

Zhu, G., Conner, S., Zhou, X., Shih, C., Brooks, H.B., Considine, E., Dempsey, J.A., Ogg, C., Patel, B., Schultz, R.M., Spencer, C.D., Teicher, B., Watkins, S.A., 2003. Synthesis of quinolinyl/isoquinolinyl [a] pyrrolo [3,4-c] carbazoles as cyclin D1/CDK4 inhibitors. Bioorg. Med. Chem. Lett. 13, 1231–1235.

JOURNAL OF VIROLOGY, May 2009, p. 5137–5147 Vol. 83, No. 10
0022-538X/09/$08.00+0 doi:10.1128/JVI.02179-08

Involvement of Creatine Kinase B in Hepatitis C Virus Genome Replication through Interaction with the Viral NS4A Protein[▽]

Hiromichi Hara,[1,2] Hideki Aizaki,[1] Mami Matsuda,[1] Fumiko Shinkai-Ouchi,[3] Yasushi Inoue,[1,4] Kyoko Murakami,[1] Ikuo Shoji,[1,5] Hayato Kawakami,[6] Yoshiharu Matsuura,[7] Michael M. C. Lai,[8] Tatsuo Miyamura,[1] Takaji Wakita,[1] and Tetsuro Suzuki[1]*

Department of Virology II[1] and Department of Biochemistry and Cell Biology,[3] National Institute of Infectious Diseases, Tokyo 162-8640, Japan; Department of Internal medicine, Division of Pulmonary Diseases, The Jikei University School of Medicine, Tokyo 105-8461, Japan[2]; Mita Hospital, International University of Health and Welfare, Tokyo 108-8329, Japan[4]; Division of Microbiology, Kobe University Graduate School of Medicine, Hyogo 650-0017, Japan[5]; Department of Anatomy, Kyorin University School of Medicine, Tokyo 181-8611, Japan[6]; Research Institute for Microbial Diseases, Osaka University, Osaka 565-0871, Japan[7]; and Department of Molecular Microbiology and Immunology, University of Southern California, Keck School of Medicine, Los Angeles, California 90033[8]

Received 15 October 2008/Accepted 20 February 2009

Persistent infection with hepatitis C virus (HCV) is a major cause of chronic liver diseases. The aim of this study was to identify host cell factor(s) participating in the HCV replication complex (RC) and to clarify the regulatory mechanisms of viral genome replication dependent on the host-derived factor(s) identified. By comparative proteome analysis of RC-rich membrane fractions and subsequent gene silencing mediated by RNA interference, we identified several candidates for RC components involved in HCV replication. We found that one of these candidates, creatine kinase B (CKB), a key ATP-generating enzyme that regulates ATP in subcellular compartments of nonmuscle cells, is important for efficient replication of the HCV genome and propagation of infectious virus. CKB interacts with HCV NS4A protein and forms a complex with NS3-4A, which possesses multiple enzyme activities. CKB upregulates both NS3-4A-mediated unwinding of RNA and DNA in vitro and replicase activity in permeabilized HCV replicating cells. Our results support a model in which recruitment of CKB to the HCV RC compartment, which has high and fluctuating energy demands, through its interaction with NS4A is important for efficient replication of the viral genome. The CKB-NS4A association is a potential target for the development of a new type of antiviral therapeutic strategy.

Hepatitis C virus (HCV) infection represents a significant global healthcare burden, and current estimates suggest that a minimum of 3% of the world's population is chronically infected (4, 19). The virus is responsible for many cases of severe chronic liver diseases, including cirrhosis and hepatocellular carcinoma (4, 16, 19). HCV is a positive-stranded RNA virus belonging to the family *Flaviviridae*. Its ~9.6-kb genome is translated into a single polypeptide of about 3,000 amino acids (aa), in which the nonstructural (NS) proteins NS2, NS3, NS4A, NS4B, NS5A, and NS5B reside in the C-terminal half region (6, 34, 44). NS4A, a small 7-kDa protein, functions as a cofactor for NS3 to enhance NS3 enzyme activities such as serine protease and helicase activities. The hydrophobic N-terminal region of NS4A, which is predicted to form a transmembrane α-helix, is responsible for membrane anchorage of the NS3-4A complex (8, 44, 50), and the central region of NS4A is important for the interaction with NS3 (10, 44). A recent study demonstrated the involvement of the C terminus of NS4A in the regulation of NS5A hyperphosphorylation and viral replication (28).

The development of HCV replicon technology several years ago accelerated research on viral RNA replication (7, 44). Furthermore, a robust cell culture system for propagation of infectious HCV particles was developed using a viral genome of HCV genotype 2a, JFH-1 strain, enabling us to study every process in the viral life cycle (27, 47, 54). RNA derived from genotype 1a, HCV H77, containing cell-culture adaptive mutations, also produces infectious viruses (52). Using these systems, it has been reported that the HCV genome replicates in a distinct, subcellular replication complex (RC) compartment, which includes NS3-5B and the viral RNA (2, 14, 33). The RC forms in a distinct compartment with high concentrations of viral and cellular components located on detergent-resistant membrane (DRM) structures, possibly a lipid-raft structure (2, 41), which may protect the RC from external proteases and nucleases. Almost all processes in viral replication are dependent on the host cell's machinery and involve intimate interaction between viral and host proteins. However, the functional roles of host factors interacting with the HCV RC in viral genome replication remain ambiguous.

To gain a better understanding of cellular factors that are components of the HCV RC and that function as regulators of viral replication, a comparative proteomic analysis of DRM fractions from HCV replicon and parental cells and subsequent RNA interference (RNAi) silencing of selected genes were performed. We identified creatine kinase B (CKB) as a key factor for the HCV genome replication. CKB catalyzes the reversible transfer of the phosphate group of phosphocreatine

* Corresponding author. Mailing address: Department of Virology II, National Institute of Infectious Diseases, 1-23-1 Toyama, Shinjuku-ku, Tokyo 162-8640, Japan. Phone: 81-3-5285-1111. Fax: 81-3-5285-1161. E-mail: tesuzuki@nih.go.jp.
[▽] Published ahead of print on 4 March 2009.

(pCr) to ADP to yield ATP and creatine and is known to play important roles in local delivery and cellular compartmentalization of ATP (48, 51). The findings obtained here suggest that recruitment of CKB to the HCV RC, through CKB interaction with NS4A, is essential for maintenance or enhancement of viral replicase activity.

MATERIALS AND METHODS

Cell lines, antibodies, and reagents. Human hepatoma cell line Huh-7.5.1 (54) was kindly provided by Francis V. Chisari. Cell lines carrying subgenomic replicon RNAs, namely, SGR-N (41) and SGR-JFH1 (23), were derived from the HCV-N (17) and JFH-1 strains (24), respectively. Mouse monoclonal antibodies (MAbs) against HCV NS3 (Chemicon, Temecula, CA), NS4A (Santa Cruz Biotechnology, Inc., Santa Cruz, CA), NS5A (Biodesign, Saco, ME), NS5B (2), FLAG (M2; Sigma-Aldrich, St. Louis, MO), glyceraldehyde-3-phosphate dehydrogenase (GAPDH; Chemicon), and Flotillin-1 (BD Biosciences, San Jose, CA) and polyclonal antibodies (PAbs) against CKB (mouse [Abnova, Taipei, Taiwan], goat [Santa Cruz]), hemagglutinin (HA; Sigma-Aldrich), and FLAG (Sigma-Aldrich) were used. Cyclocreatine (Ccr; also known as 2-imino-1-imidazolidineacetic acid), pCr, and phosphopyruvic acid (pPy) were purchased from Sigma-Aldrich. Recombinant CKB and pyruvate kinase (PK) were obtained from Acris (Herfold, Germany) and Calbiochem (San Diego, CA), respectively.

Proteome analysis. RC-rich membrane fractions of cells were isolated as described previously (2, 41). Briefly, cells were lysed in hypotonic buffer. After removing the nuclei, supernatants were treated with 1% NP-40 for 60 min, mixed with 70% sucrose, overlaid with 55 and 10% sucrose, and centrifuged at 38,000 rpm for 14 h. Proteins from membrane fractions were purified by using a 2D Clean-Up kit (GE Healthcare, Tokyo, Japan), followed by labeling with fluorescent dyes: Cy5 for replicon cells, Cy3 for parental cells, and Cy2 for the protein standard containing equal amounts of both cell samples. Two-dimensional fluorescence difference gel electrophoresis (2D-DIGE) was performed using Immobiline DryStrip as the first-dimension gel and 12.5% polyacrylamide gel as the second-dimension gel. The 2D-DIGE images were analyzed quantitatively using the DeCyder software (GE Healthcare). Student *t* test was performed on differences between the tested samples using DeCyder biological variation analysis module. Samples were analyzed in triplicate. The protein spots of interest were excised from the gel, subjected to in-gel digestion using trypsin or lysyl endopeptidase and analyzed by liquid chromatography (MAGIC 2002 System; Michrom Bioresources, Auburn, CA) directly connected to electrospray ionization-ion trap mass spectrometry (LCQ-decaXP; Thermo Electron Corp., Iwakura, Japan). The results were subjected to database (NCBInr) search by Mascot server software (Matrix Science, Boston, MA) for peptide assignment.

Plasmids. A human CKB cDNA (43; kindly provided by Oriental Yeast Corp., Tokyo, Japan) was inserted into the EcoRI site of pCAGGS, yielding pCAGCKB. To generate expression plasmids for HA-tagged versions of wild-type and deletion mutated CKB, the corresponding DNA fragments were amplified by PCR, followed by introduction into the BglII site of pCAGGS. A fragment representing the inactive mutant CKB-C283S was synthesized by PCR mutagenesis. To generate FLAG-tagged NS protein expression plasmids, DNA fragments encoding either NS3, NS4A, NS4B, NS5A, or NS5B protein were amplified from HCV strains NIHJ1 (1) and JFH-1 (23) by PCR, followed by cloning into the EcoRI-EcoRV sites of pcDNA3-MEF (20). To generate an HA-tagged NS3 expression plasmid, a fragment encoding NS3 with the HA tag sequence at its N terminus was inserted into pCAGGS.

siRNA transfection. The small interfering RNAs (siRNAs) targeted to CKB (CKB-1 [5′-UAAGACCUUCCUGGUGUGGTT-3′] and CKB-2 [5′-CGUCAC CCUUGGUAGAGUUTT-3′]) and the scramble negative control siRNA to CKB-2 (5′-GGCGUACUAGCUUAUUCGCTT-3′) were purchased from Sigma. Cells in a 24-well plate were transfected with siRNA using HiPerFect transfection reagent (Qiagen, Tokyo, Japan) according to the manufacturer's instructions. The siRNA sequences for the other genes used in the siRNA screening are available upon request.

HCV infection. Culture media from Huh-7 cells transfected with in vitro-transcribed RNA corresponding to the full-length JFH-1 (47) was collected, concentrated, and used for the infection assay (3).

Quantification of HCV core protein and RNA. To estimate the levels of HCV core protein, aliquots of culture supernatants or of cell lysates were assayed by using HCV Core enzyme-linked immunosorbent assay kits (5). Total RNA was isolated from harvested cells using TRIzol (Invitrogen, Carlsbad, CA). Copy numbers of the viral RNA were determined by reverse transcription-PCR (RT-PCR) (2, 36, 46).

Immunoprecipitation, immunoblot analysis, and immunofluorescence microscopy. The analyses, as well as DNA transfection, were performed essentially as previously described (42). Cells were lysed in immunoprecipitation lysis buffer (50 mM Tris-HCl [pH 7.6], 150 mM NaCl, 1% sodium deoxycholate, 1% NP-40, 0.1% sodium dodecyl sulfate, 1 mM dithiothreitol, 1 mM calcium acetate). For immunoprecipitation, supernatants of cell lysates were precipitated with anti-FLAG antibody and protein A-Sepharose Fast Flow beads (GE healthcare). For immunofluorescence microscopy, anti-CKB goat PAb and anti-NS4A MAb as primary antibodies and Alexa Fluor 555-conjugated donkey anti-goat immunoglobulin G (Invitrogen) and Alexa Fluor 488-conjugated rabbit anti-mouse immunoglobulin G (Invitrogen) as secondary antibodies were used and observed under an LSM 510 confocal microscope (Carl Zeiss, Oberkochen, Germany).

Immunoelectron microscopy. Postembedding immunostaining using the colloidal gold-labeling method was performed as described previously (38). Cells were fixed in 4% paraformaldehyde–1% glutaraldehyde at 4°C for 1 h. After dehydration through a graded series of ethanol, cells were embedded in LR White (London Resin Company, London, United Kingdom) and sectioned. After blocking, section grids were incubated with a mixture of anti-NS4A and anti-CKB antibodies at 4°C overnight, followed by treatment with a mixture of 18-nm colloidal gold-conjugated donkey anti-mouse immunoglobulin G and 12-nm colloidal gold-conjugated donkey anti-goat immunoglobulin G antibodies (Jackson Immunoresearch, West Grove, PA) at 4°C overnight. The sections were stained with uranyl acetate and observed under a transmission electron microscope.

Measurement of CK activity and cellular ATP level. Cells were lysed with passive lysis buffer (Promega, Madison, WI), and CK activities were measured based on Oliver methods (40), in which the activity of converting creatine phosphate and ADP to creatine and ATP was measured. ATP levels in cell lysates were measured by using a CellTiter-Glo luminescent cell viability assay (Promega).

RNA replication assays in permeabilized replicon cells and in vitro. The RNA synthesis assay using permeabilized replicon cells was based on a previously described method (33). Briefly, SGR-JFH1 cells were treated with 5 μg of actinomycin D/ml for 2 h, followed by permeabilization with 50 μg of digitonin/ml for 5 min. The resulting mix was incubated with 500 μM concentrations of ATP, GTP, and CTP; 10 μCi of UTP ([α-^{32}P]UTP); 50 μg of actinomycin D/ml; and 5 mM pCr with or without 20 U of CKB/ml for 4 h at 27°C. RNA was extracted by using TRIzol and analyzed by 1% formaldehyde agarose gel electrophoresis. The cell-free RNA replication assay was performed as described previously (2).

In vitro helicase assays. Helicase activity on double-stranded RNA (dsRNA) was investigated as described previously (11) with some modifications. The 5′ end of the release strand was labeled with [γ-^{32}P]ATP using T4 polynucleotide kinase (Ambion). The dsRNA substrate was obtained by annealing the labeled RNA with a template strand RNA at a molar ratio of 1:1. The helicase assay mixture contained 5 nM dsRNA, helicase enzyme (80 nM NS3 or NS3-4A [kindly provided by R. De Francesco]), 6 mM ATP, in the presence or absence of 20 U of CKB/ml in an assay buffer (25 mM MOPS-NaOH [pH 7.0], 2.5 mM dithiothreitol, 100 μg of bovine serum albumin/ml, 3 mM $MgCl_2$, 5 mM pCr, 2.5 U of RNase inhibitor/ml). After the helicase reaction, samples were electrophoresed in a native 8% polyacrylamide gel and autoradiographed.

To determine the effect of PK/pPy system on the helicase activity, PK and pPy were used instead of CKB and pCr. Helicase activity on dsDNA was measured based on homogeneous time-resolved fluorescence quenching using a Trupoint helicase assay kit (Perkin-Elmer, Waltham, MA) according to the manufacturer's instructions.

In vitro protease assay. In vitro HCV protease activity of NS3-4A or NS3 was analyzed by using a SensoLyteHCV protease assay kit (AnaSpec, San Jose, CA) according to the manufacturer's instructions.

RESULTS

Identification of host factors involved in HCV RNA replication by comparative proteomic analysis of DRM fractions and RNAi silencing. To identify host proteins involved in the HCV RC, proteome profiles of the RC-rich membrane fraction in Huh-7 cells harboring subgenomic replicon RNA derived from genotype 1b, N isolate (SGR-N) were compared to those of parental cells by 2D-DIGE. We confirmed that the DRM fraction obtained from SGR-N cells is functionally active in a

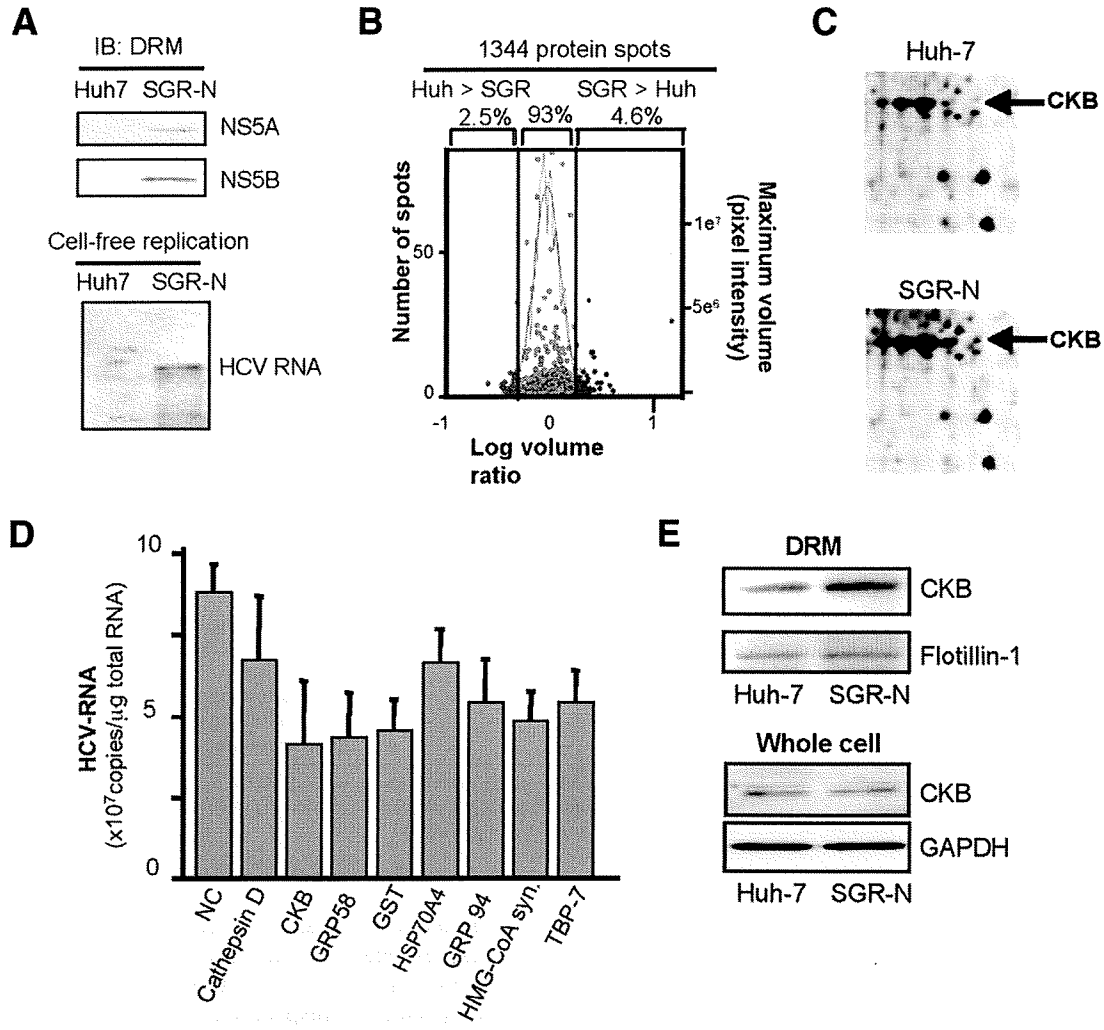

FIG. 1. Comparative proteomic analysis of DRM fractions and RNAi silencing. (A) Preparation of functionally active RC fraction for proteome analysis. DRM fractions obtained from SGR-N cells and parental Huh-7 cells were analyzed by immunoblotting with anti-NS5A and anti-NS5B antibodies (upper panel) and by the cell-free RNA replication assay (lower panel). (B) Histogram representation of proteins detected in 2D-DIGE. Images were analyzed quantitatively by the DeCyder software. The left and right *y* axis, respectively, indicate the spot frequency and the maximum volume of each spot, given against the log volume ratio (*x* axis). (C) Comparison of 2D-DIGE maps of proteins from DRM fractions of SGR-N cells and Huh-7 cells. Enlarged 2D-DIGE gel images of regions containing protein spots of CKB (arrows) are shown. (D) Effects of siRNAs of genes selected from comparative proteome analysis on HCV RNA replication. SGR-N cells were transfected with siRNA specific to cathepsin D, CKB (siCKB-1), GRP58, GST, Hsp70 protein 4, GRP94, HMG-coenzyme A synthase, or Tat binding protein 7 or with nontargeting (NC) siRNA. At 48 h posttransfection, total RNA was isolated and HCV RNA levels were assessed by real-time RT-PCR. (E) Enrichment of CKB in the DRM of HCV replicon cells. Equal amounts of DRM fractions from SGR-N and parental Huh-7 cells, or whole-cell lysates from both cells were analyzed by immunoblotting with antibodies against CKB, flotilin-1 or GAPDH.

cell-free replication assay (Fig. 1A). Three independent proteome experiments were performed for a reliable analysis of protein expression. Approximately 1,300 spots were resolved in each gel, and 4 to 5% of the protein spots represented a >2-fold increase in the membrane fraction of replicon cells in each experiment (Fig. 1B). The protein spots that exhibited high reproducibility (an example shown in Fig. 1C) were excised, digested by trypsin or lysyl endopeptidase, and analyzed by mass spectrometry, which identified the corresponding proteins in 27 cases (Table 1). Among the proteins implicated in a variety of functional categories, 10 were involved in protein folding, mainly as chaperones, 7 were metabolic and biosynthesis enzymes including proteins for redox regulation or energy pathways, 3 were involved in cytoskeleton organization, and 3 proteins were related to cellular processes, mainly proteolysis pathways. The viral NS proteins identified as differentially expressed proteins in the analysis were not listed.

In order to identify host factors involved in HCV replication, we examined the effects on viral RNA replication of transfection of SGR-N cells with siRNAs against genes encoding nine proteins belonging to diverse classes of biological functions (Table 1). Each siRNA reduced the HCV RNA level to 47 to 76% of the level of the siRNA control (Fig. 1D). None of the siRNAs tested exhibited considerable cytotoxicity against the replicon cells, ruling out overt toxicity as a mechanism for inhibition of viral RNA replication. Among the candidate

TABLE 1. Selected proteins that reproducibly increased in the DRM fraction of SGR-N cells[a]

Avg ratio	*P* (Student *t* test)	Coverage (%)	Protein name	Molecular function	GI no.
5.56	0.04	27	GRP94	Protein folding	15010550
4.99	0.07	47	Hsp60	Protein folding	6996447
3.73	0.07	6	tRNA guanine transglycosylase	Metabolism	30583205
3.56	0.06	23	KIAA0088	Unknown	577295
3.32	0.07	4	Thioredoxin-related protein	Unknown	20067392
3.32	0.13	12	Tat binding protein 1 (TBP-1)	Cellular processes	20532406
3.06	0.14	22	Aldehyde dehydrogenase 1	Metabolism	2183299
3.06	0.14	14	Chaperonin TRiC/CCT, subunit 2	Protein folding	54696794
2.96	0.04	14	Heat shock 70-kDa protein 4 (HSPA4)	Protein folding	6226869
2.96	0.04	29	GRP58	Metabolism/protein folding	2245365
2.94	0.01	37	Mutant β-actin	Cytoskeleton organization	28336
2.65	0.17	33	Glutathione S-transferase (GST)	Catalytic activity	2204207
2.53	0.04	37	Keratin 19	Cytoskeleton organization	6729681
2.46	0.08	6	Heterogeneous nuclear ribonucleoprotein K	Nucleic acid modification	460789
2.45	0.001	13	HMG-coenzyme A synthase	Metabolism	30009
2.4	0.02	31	CKB	Energy pathway/metabolism	180570
2.4	0.02	11	Cathepsin D	Cellular processes	30582659
2.4	0.02	11	C8orf2	Unknown	37181322
2.36	0.1	38	Tropomyosin 4-anaplastic lymphoma kinase fusion protein	Cytoskeleton organization	14010354
2.36	0.1	6	Calreticulin	Protein folding	30583735
2.33	0.01	29	Quinolinate phosphoribosyltransferase	Metabolism	30583301
2.29	0.04	25	Protein disulfide isomerase-related protein 5	Protein folding	1710248
2.29	0.04	16	Tat binding protein 7 (TBP-7)	Cellular processes	263099
2.05	0.11	24	Calumenin	Metabolism	2809324
2.05	0.12	10	TRiC/CCT, subunit 5	Protein folding	24307939
2.03	0.07	20	Hsp90 beta	Protein folding	34304590
2.01	0.07	10	TRiC/CCT, subunit 1	Protein folding	36796

[a] The spectra obtained by tandem mass spectrometry were collected using data-dependent mode, and the results were subjected to database (NCBInr) search by Mascot server software (Matrix Science, London, United Kingdom) for peptide assignment. Coverage, the ratio of the portion of protein sequence covered by matched peptides to the whole protein sequence. GI no., GenInfo identifier number.

genes examined, we observed a reproducible inhibition of HCV RNA replication by two independent siRNAs targeting CKB (see below).

CKB participates in HCV RNA replication and the propagation of infectious virus. CKB is a brain-type creatine kinase isoenzyme and is also detected in a variety of other tissues, including human liver (32). Steady-state levels of CKB in the DRM fraction, as well as in whole-cell lysate of SGR-N cells were compared to those from parental cells by Western blotting. The CKB level in the DRM fraction of replicon cells was higher than that in parental cells (Fig. 1E), confirming the results of the proteome analysis described above. In contrast, the CKB level in whole cells was similar in both cells (Fig. 1E). These results suggest participation of posttranslational modification, such as translocation to the DRM fraction, of CKB in replicon cells.

Figure 2A shows the inhibitory effect on HCV RNA replication of CKB siRNA; siCKB-2, the sequence of which does not overlap with the sequence of siCKB-1 used in the above siRNA screening (Fig. 1D). Transfection with siCKB-2 effectively decreased the cellular level of CKB enzymatic activity (data not shown), as well as the abundance of CKB protein (Fig. 2A), and resulted in 60% reduction in the viral RNA level in SGR-N cells compared to the cells treated with control siRNA. This inhibitory effect of siRNA on HCV RNA abundance was also observed in JFH-1-derived subgenomic replicon (SGR-JFH1) cells. The viral RNA level in the cells transfected with siCKB-2 decreased by 50% compared to the control (Fig. 2A). We also tested the CKB mutant, CKB-C283S, in which Cys at aa 283, near the catalytic site, has been replaced with Ser (Fig. 3A) and which is known to be enzymatically inactive and to work in a dominant-negative manner (22, 29). As expected, overexpression of CKB-C283S resulted in a reduction in HCV RNA replication in SGR-N cells (Fig. 2B). We obtained a similar result in SGR-JFH1 cells, as described below (Fig. 3E).

To further examine the involvement of CKB in HCV RNA replication, we tested the effect of Ccr, a substrate analogue and possible inhibitor for CK in either SGR-N, SGR-JFH1 (Fig. 2C), or Huh7 cells transiently replicating luciferase-subgenomic replicon (data not shown). We found dose-dependent inhibition of HCV RNA replication but no observed effect on total cellular levels of protein and ATP (Fig. 2D) in the replicon setting used.

We next examined whether the knockdown of CKB or treatment with Ccr would abrogate the production of HCVcc. At 72 h posttransfection with siCKB-2, the HCV core level in cells infected with HCVcc was significantly reduced (Fig. 2E). Treatment of the infected cells with Ccr at various concentrations also reduced the intracellular and supernatant core level and subsequently decreased HCVcc production (Fig. 2F). These results demonstrate that suppression of the HCV RNA replication by the siRNA-mediated knockdown of CKB or treatment with CKB inhibitor leads to reduction of the production of infectious virus.

CKB interacts with HCV NS4A. Having established a role for CKB in HCV RNA replication, we then tried to determine to how CKB influences the HCV life cycle. It has been re-

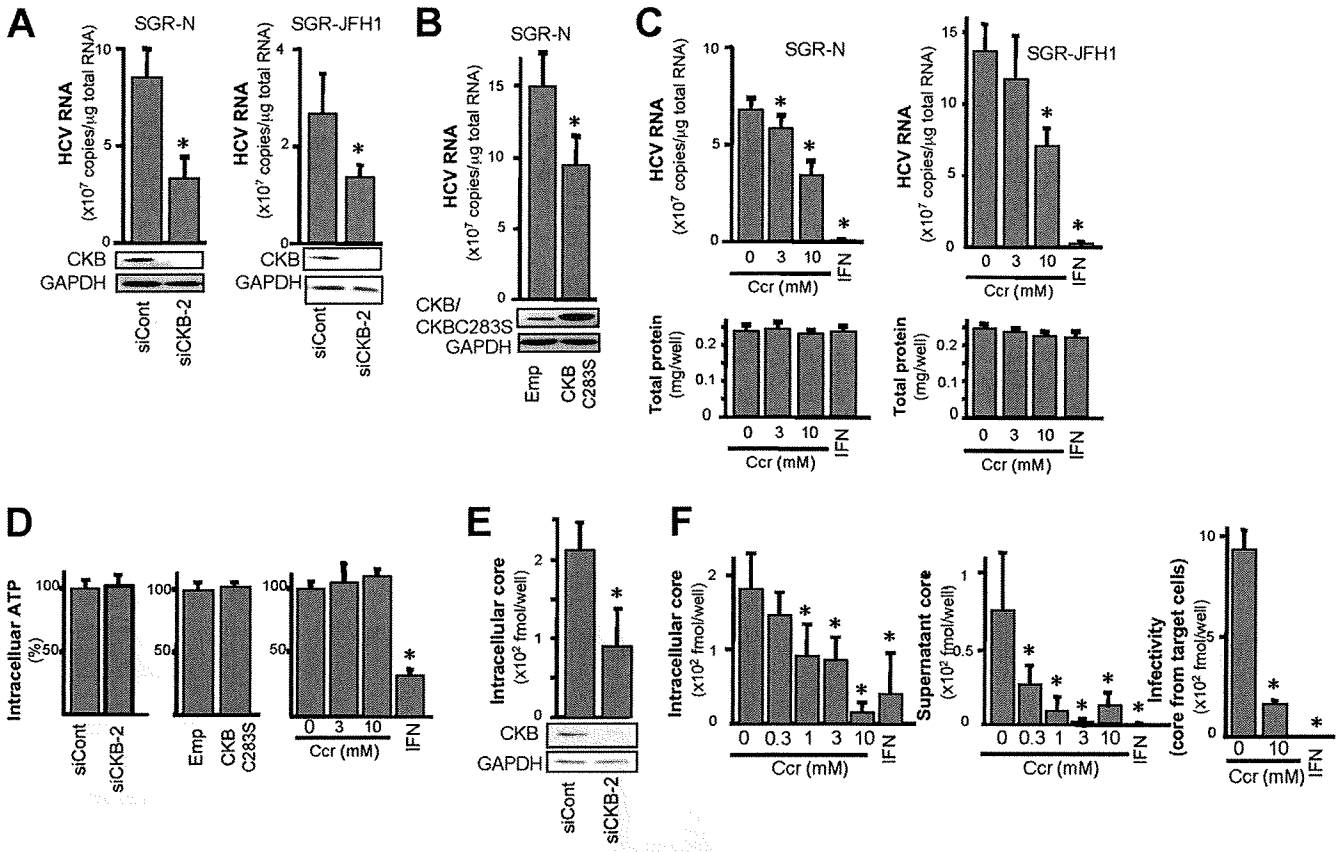

FIG. 2. Involvement of CKB in HCV replication. (A and E) Knockdown of endogenous CKB in SGR-N and SGR-JFH1 cells (A) or HCVcc-infected cells (E). Cells were transfected with siRNA against CKB (siCKB-2) or control siRNA (siCont) and were harvested at 72 h posttransfection. Real-time RT-PCR for HCV RNA levels and immunoblotting for CKB and GAPDH were performed. (B) SGR-N cells were transfected with pCAGCKB-C283S or empty vector, and HCV RNA levels and expression of CKB and CKB-C283S were determined 72 h posttransfection. SGR-N and SGR-JFH1 cells (C) or HCVcc-infected cells (F) were treated with Ccr at various concentrations for 72 h, followed by quantification of HCV RNAs and total cellular proteins. ATP levels (D) were determined after transfection with siCKB-2, pCAGCKB-C283S, or treatment with Ccr for 72 h in SGR-N cells. The ATP levels in the cells transfected with negative control siRNA (left), empty vector (middle), and no treatment (right) were set at 100%, respectively. (F) HCVcc-infected cells were treated with Ccr, and the viral core protein levels in cells (left) and supernatants (middle) were determined at 72 h postinfection. Collected culture supernatants were inoculated into naive Huh-7.5.1 cells after the removal of Ccr. After 72 h, the core proteins in cells were determined (right panel). All data are presented as averages and standard deviation values for at least triplicate samples. *, $P < 0.05$ against control such as transfection with siCont (A and E) or empty vector (B) or nontreatment (C, D, and F).

ported that interaction of CKB with some cellular proteins is required for local availability of CKB activity and local generation of ATP (22, 29). To examine the possible interaction of CKB with HCV NS proteins, HA-tagged CKB (HA-CKB) was coexpressed with FLAG-tagged NS proteins (NIHJ1 strain), followed by immunoprecipitation with an anti-FLAG antibody. CKB was shown to specifically interact with NS4A. No or little interaction was observed between CKB and either NS3, NS4B, NS5A, or NS5B (Fig. 3B). CKB-NS4A interaction was also found with the JFH-1 strain (Fig. 3C).

To identify the CKB region required for the interaction with NS4A, various deletion mutants of CKB were generated (Fig. 3A). An immunoprecipitation assay indicated that NS4A was coimmunoprecipitated with either a full-length CKB, a C-terminal deletion (aa 1 to 357), an N-terminal deletion (aa 297 to 381), or CKB-C283S, but not with aa 1 to 296, aa 1 to 247, or aa 1 to 184 (Fig. 3D, upper middle panel). Further, internal deletions of CKB (CKBdel297-357 and CKB-C283Sdel297-357) failed to interact with NS4A (Fig. 3D, lower panel), suggesting that aa 297 to 357 of CKB are important for its interaction with NS4A. It is noted that the expression of CKB aa 297 to 357 in cells was undetected, presumably due to its misfolding and/or instability. To verify a role for CKB-NS4A interaction in HCV RNA replication, we further determined the effect of expression of either CKB-C283S or its internal deletion lacking aa 297 to 357 (CKB-C283Sdel297-357) on viral replication in SGR-JFH1 cells. As expected, the HCV RNA level was significantly decreased by CKB-C283S, whereas this effect was not observed by CKB-C283Sdel297-357 (Fig. 3E).

NS4A is a 54-residue small protein composed of three domains: the N-terminal membrane anchor, the central domain responsible for interacting with NS3, and the C-terminal acidic domain. To define the portion in NS4A responsible for its interaction with CKB, we constructed three NS4A deletion mutants, each separately expressing one of the NS4A domains, with a FLAG tag (Fig. 3F). CKB proved to interact with the central domain, aa 21 to 39, of NS4A, which is involved in

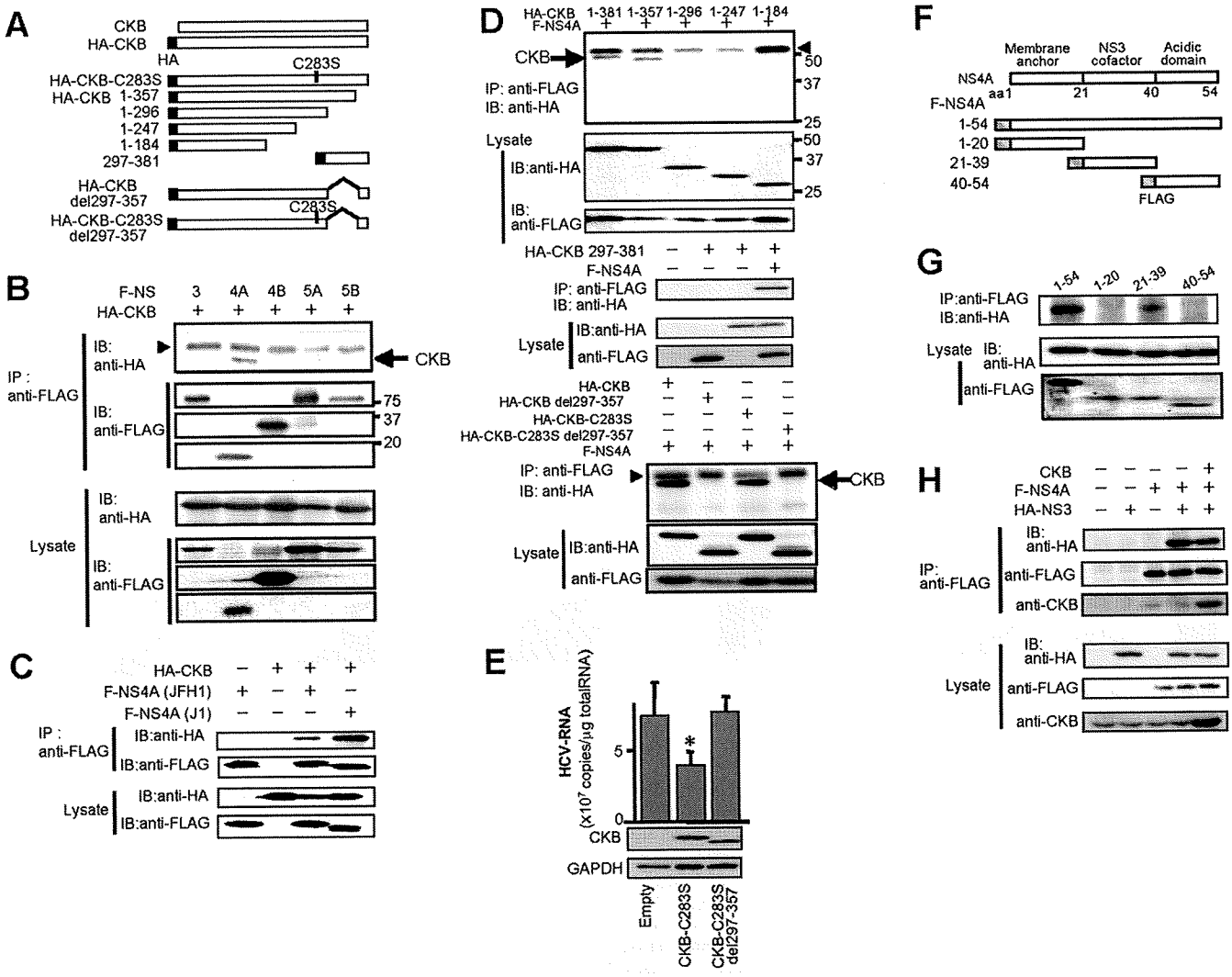

FIG. 3. CKB interacts with HCV NS4A. (A) Structures of CKB constructs used in the present study. A full-length wild-type CKB without an epitope tag (CKB) or with an N-terminal HA tag (HA-CKB), HA-CKB with deletions (aa 1 to 357, aa 1 to 296, aa 1 to 247, aa 1 to 184, and aa 297 to 381 and del297-357), CKB mutant at the catalytic site, Cys-283 (CKB-C283S) or CKB-C283S lacking aa 297 to 357 (CKB-C283Sdel297-357) are shown. HA-CKB was coexpressed with FLAG-tagged versions of each NS protein of strain NIHJ1 (B) or with NS4A of strain JFH-1 (C) in 293T cells and immunoprecipitated (IP) with an anti-FLAG antibody. Immunoprecipitates were subjected to immunoblotting (IB) with anti-HA or anti-FLAG antibody. (D) Each CKB deletion mutant was coexpressed with FLAG-NS4A in 293T cells. Immunoprecipitates were analyzed by immunoblotting. Arrow, CKB; arrowhead, immunoglobulin heavy chain. (E) SGR-JFH1 cells were transfected with the expression plasmid for CKB-C283S, CKB-C283Sdel297-357 or empty vector. At 72 h posttransfection, HCV RNA levels and the expression of CKB and CKB-C283S were determined by real-time RT-PCR and immunoblotting with anti-HA antibody, respectively. For HCV RNA quantitation, data are indicated as averages and standard deviations ($n = 3$). *, $P < 0.05$ against the empty vector control. (F) Structure of NS4A and NS4A constructs. FLAG-tagged NS4A (aa 1 to 54) or its truncated mutants (aa 1 to 20, aa 21 to 39, or aa 40 to 54) are shown. (G) Each NS4A deletion mutant was coexpressed with HA-CKB and analyzed as described above. (H) FLAG-NS4A was coexpressed with HA-NS3 or HA-NS3 and CKB, followed by immunoprecipitation with anti-FLAG antibody. Immunoprecipitates were analyzed by immunoblotting with anti-HA, anti-FLAG or anti-CKB antibody.

formation of the NS3-NS4A complex (Fig. 3G). We therefore investigate whether NS3-NS4A interaction is affected in the presence of CKB and found that exogenous expression of CKB has no influence on NS3-NS4A interaction, and a putative NS3-NS4A-CKB complex was detected in the coimmunoprecipitation analysis (Fig. 3H). Collectively, these results strongly suggest that CKB plays a key role in HCV RNA replication via interaction with NS4A.

Subcellular localization of CKB and NS4A in cells replicating HCV RNA. CKB is distributed throughout cells but is mainly localized in the perinuclear area (31), whereas NS4A is predominantly localized at the endoplasmic reticulum and mitochondrial membranes (37). We examined the possible subcellular colocalization of CKB and NS4A in SGR-N cells by immunofluorescence staining (Fig. 4A). CKB tended to gather in the perinuclear area of HCV replicating cells and was partially colocalized with NS4A in the area, sharing a dotlike structure. To further analyze the subcellular compartments in which CKB and NS4A coexist, we used double-labeling immunoelectron microscopy on SGR-N cells using antibodies against CKB and NS4A, with secondary antibodies coupled to 12- and 18-nm gold particles, respectively. One fraction of